DEVELOPMENT OF POLY(TRIMETHYLENE CARBONATE) BASED BIODEGRADABLE MICROPARTICLES

A THESIS SUBMITTED TO
THE GRADUATE SCHOOL OF NATURAL AND APPLIED SCIENCES
OF
MIDDLE EAST TECHNICAL UNIVERSITY

BY

GÖZDE ŞAHİN

IN PARTIAL FULFILLMENT OF THE REQUIREMENTS
FOR
THE DEGREE OF MASTER OF SCIENCE
IN
CHEMICAL ENGINEERING

FEBRUARY 2018

Approval of the thesis:

DEVELOPMENT OF POLY(TRIMETHYLENE CARBONATE) BASED BIODEGRADABLE MICROPARTICLES

submitted by **Gözde ŞAHİN** in partial fulfillment of the requirements for the degree of **Master of Science in Chemical Engineering Department, Middle East Technical University** by,

Prof. Dr. M. Gülbin DURAL ÜNVER _____
Dean, Graduate School of **Natural and Applied Sciences**

Prof. Dr. Halil KALIPÇILAR _____
Head of Department, **Chemical Engineering**

Asst. Prof. Dr. Erhan BAT _____
Supervisor, **Chemical Engineering Dept., METU**

Assoc. Prof. Dr. Seha TİRKEŞ _____
Co-supervisor,
Chemical Eng. and Applied Chem. Dept., Atilim University

Examining Committee Members:

Assoc. Prof. Dr. Bora MAVİŞ _____
Mechanical Engineering Dept., Hacettepe University

Asst. Prof. Dr. Erhan BAT _____
Chemical Engineering Dept., METU

Assoc. Prof. Dr. Seha TİRKEŞ _____
Chemical Eng. and Applied Chem. Dept., Atilim University

Asst. Prof. Dr. Harun KOKU _____
Chemical Engineering Dept., METU

Asst. Prof. Dr. Emre BÜKÜŞOĞLU _____
Chemical Engineering Dept., METU

Date: 01.02.2018

I hereby declare that all information in this document has been obtained and presented in accordance with academic rules and ethical conduct. I also declare that, as required by these rules and conduct, I have fully cited and referenced all material and results that are not original to this work.

Name, Last name: Gözde Şahin

Signature:

ABSTRACT

DEVELOPMENT OF POLY(TRIMETHYLENE CARBONATE) BASED BIODEGRADABLE MICROPARTICLES

Şahin, Gözde

M.Sc., Department of Chemical Engineering

Supervisor: Asst. Prof. Dr. Erhan Bat

Co-Supervisor: Assoc. Prof. Dr. Seha Tirkeş

February 2018, 77 pages

Microparticles are promising in many fields of application, such as polymeric drugs, drugs and vaccine delivery systems, cell markers because of their versatility.

Since it is important that the particles should have a certain shape and size, various fabrication methods have been tried for the production of the particles such as bottom-up and top-down methods. One of the most recent and eligible method among them is Particle Replication in Non-wetting Templates (PRINT) technique. PRINT is a top-down fabrication technique used for the production of free particles with a specific shape and size. With this technique, it has been tried to produce particles from polymers that are used frequently in biomedical applications. Recently, poly(trimethylene carbonate) (PTMC) has become a prominent biomaterial due to its unique properties when compared to widely used polymers. In this study, PTMC based micro carriers were produced using the PRINT technique. Therefore, PTMC oligomers were synthesized by ring opening polymerization. The end group of the oligomers were double bonded with methacryloyl chloride so that the synthesized oligomers could be fabricated

as particles of a certain shape and size. In order to apply the PRINT technique, masks with protruded patterns have been prepared with standard lithographic methods. With the help of these masks, non-wetting surface PFPE molds with indented patterns were created. The synthesized PTMC oligomers were poured onto the mold and crosslinked to take the shape of the mold cavities.

The free particles produced were collected by the non-wetting surface of the mold, and their morphological characteristics were examined by scanning electron microscope (SEM) imaging technique. According to the results, rectangular particles with dimensions of 2 μm x 8 μm, and cylindrical and cubic PTMC based particles ranging from 2-100 μm were produced.

Keywords: Microparticle, top-down fabrication, poly(trimethylene carbonate), PRINT

ÖZ

POLİ(TRİMETİLEN KARBONAT) ESASLI BİYOBOZUNUR MİKROPARÇACIKLARIN GELİŞTİRİLMESİ

Şahin, Gözde
Yüksek Lisans, Kimya Mühendisliği Bölümü
Tez Yöneticisi: Yrd. Doç. Dr. Erhan Bat
Ortak Tez Yöneticisi: Doç. Dr. Seha Tirkeş

Şubat 2018, 77 sayfa

Mikroparçacıklar çok yönlü malzemeler olmaları nedeniyle, polimerik ilaç, ilaç ve aşı taşıyıcı sistem, hücre işaretleyici gibi birçok uygulama alanlarında gelecek vaat ederler. Kullanılan parçacıkların belirli bir şekil ve boyuta sahip olması önemli olduğundan parçacık üretimi için aşağıdan yukarı ve yukarıdan aşağı olmak üzere farklı fabrikasyon metotları denenmiştir. Bu fabrikasyon teknikleri arasında en yeni ve etkili metotlardan biri de Particle Replication in Non-wetting Templates (PRINT) tekniğidir. PRINT; belirli bir şekli ve boyutu olan, serbest parçacık üretimi için kullanılan yukarıdan aşağıya fabrikasyon tekniğidir. Bu teknikle şimdiye kadar biyomedikal uygulamalarda çok sık kullanılan polimerlerden parçacık üretilmesi denenmiştir. Ancak, son zamanlarda öne çıkan poli(trimetilen karbonat) (PTMC), yaygın olarak kullanılan polimerlerle karşılaştırıldığında özgün özellikleri sayesinde öne çıkan bir biyomalzeme olmuştur. Bu çalışmada, PRINT tekniği kullanılarak PTMC esaslı mikrotaşıyıcılar üretilmiştir. Bunun için, PTMC oligomerleri halka açılma polimerizasyonu ile sentezlenmiştir. Sentezlenen oligomerlerin belirli bir şekle

ve boyuta sahip parçacıklar olarak üretilebilmesi için uçları metakriloil klorür ile çift bağlı hale getirilmiştir. PRINT tekniğinin uygulanabilmesi için, standard litografik yöntemlerle, belirli boyutlarda çıkıntılı desenlere sahip maskeler hazırlanmıştır. Bu maskeler yardımıyla, girintili desenlere sahip yapışmaz yüzeyli PFPE kalıplar oluşturulmuştur. Sentezlenen PTMC oligomerleri kalıp içerisine dökülüp çapraz bağlanarak kalıp boşluklarının şeklini alması sağlanmıştır.

Üretilen serbest parçacıkların, kalıbın yapışmaz yüzeyi sayesinde toplandıktan sonra taramalı electron mikroskopu (SEM) görüntüleme tekniği ile morfolojik özellikleri incelenmiştir. Elde edilen sonuçlara göre, boyutları 2 μm x 8 μm olan dikdörtgen parçacıklar ile 2-100 μm arasında değişen silindirik ve kübik PTMC esaslı parçacıklar üretilmiştir.

Anahtar Kelimeler: Mikroparçacık, yukarıdan-aşağı fabrikasyon, politrimetilen karbonat, PRINT

To my beloved parents,

ACKNOWLEDGMENTS

There are many people to whom I wish to convey my heartfelt gratitude. First, I would like to express my sincere appreciation and gratitude towards my supervisor Asst. Prof. Dr. Erhan Bat for his guidance, support and giving me a chance to work with him in such an exciting project and inspiring environment.

My sincere thanks go to Assoc. Prof. Dr. Seha Tirkeş for his advice and encouragement. He has not only been a co-supervisor, but has also been a great friend.

I would also like to express my special thanks to Prof. Dr. Atilla Cihaner, who has always been willing to listen or advise as necessary. I appreciate him for having provided the use of his laboratory facilities in Atilim University. Also, I am thankful to Dr. Salih Ertan for his very valuable friendship and continuous help in every possible way. I cannot tell you all how much I learned from you!

Additionally, I would like to thank Asst. Prof. Dr. Samad Nadimi Bavil Oliaei for his kind concern, consideration and suggestions regarding my future career.

I would like to express my thankful to METU Central Laboratory staff especially Kaan Kirdeciler for his limitless help during analysis. Also, I am grateful to Süha Tirkeş for his assistance in Scanning Electron Microscopy Analysis.

I owe a big thank you to the faculty members of Chemical Engineering and Applied Chemistry Department at the Atilim University, especially Assoc. Prof. Dr. Belgin İşgör for keeping me alive, trying her best to create a great atmosphere at work and deep understanding and advices about life. I am forever grateful for her support and motivation! I also thank to Asst. Prof. Dr. Hakan Kayı and Asst. Prof. Dr. Enver Güler for their tolerance and sincerity.

During my graduate program, I have had the good fortune of working closely with many truly gifted and dedicated colleagues in Atilim University: Zuhal Selvi Vanlı Güner, Elif Demir and Tuğçe Gültan. I wish to thank for their great support, and help during my studies, very close friendships, kind suggestions especially for future. Moreover, special thanks to Kayacan Kestel, Nil Akdede

and Niyazi Şenol. They have helped to make assistantship more enjoyable and become faithful friends whenever I need. I am also grateful to Erhan Akan, Semiha Şener, Sevilay Sevgi and Tarık Çelik for the many happy moments that we had together.

I was also fortunate to have had the support and friendship of many people in the Bat Lab and other research labs in Chemical Engineering Department, METU over the years. Thanks especially to Aslı Karausta, Berrak Erkmen, Burak Akdeniz, Cansu Çaylan, Duygu Sezen Polat, Elif Kıratlı, Ezgi Yavuzyılmaz, Hatice Özyetiş, Öznur Doğan, Seda Sivri, Sibel Öztürk and Zeynep Cansu Özçınar. It would not be possible for me to list all of their names and the memories they have provided over years in the acknowledgments but I would have to at least mention about Esranur Yıldıran, Özge Erdem and Selda Odabaşı. I express my sincere thanks to them for being such true friends, whom I could always count on. Thank you for keeping me sane during graduate school with visits, calls, encouragement, and advice.

The last but not the least, I would like to express my deepest thanks to my parents Selma & Tahir Şahin for their life-long, unconditional love throughout my life. Thank you for always encouraging me to go after my dreams. I literally could not have done this without your help! My beloved sister and brother - I know living apart has not been easy, and I am so grateful your patience. To my sister, Selin – thanks for being like an alarm clock every morning. It was quite motivating to wake up in the morning with your cheerful voice. To my brother, Doruk – you always know how to make me laugh. I am very grateful to both of you for your support and friendship, they mean the world to me. Thank you so much!

TABLE OF CONTENTS

LIST OF TABLES

TABLES

LIST OF FIGURES

FIGURES

NOMENCLATURE

ALD	Atomic layer deposition
CVD	Chemical vapor deposition
$CDCl_3$	Deuterated chloroform
EBL	Electron beam lithography
GPC	Gel permeation chromatography
T_g	Glass transition temperature
MC	Methacryloyl chloride
MEC	Minimum effective concentration
MTC	Minimum toxic concentration
MBE	Molecular beam epitaxy
NIL	Nanoimprint lithography
Mn	Number average molecular weight
PRINT	Particle Replication in Non-wetting Templates
Pep	Peptide
PFPE	Perfluoropolyether
PI	Photoinitiator
PLA	Poly(D-lactic acid)
PDMS	Poly(dimethylsiloxane)
PEG	Poly(ethylene glycol)
Pglu	Poly(glutamic acid)
PGA	Poly(glycolic acid)
PLG	Poly(lactide-co-glycolide)
PLGA	Poly(lactide-co-glycolide)
PPy	Poly(pyrrole)
PS	Poly(styrene)
PVA	Poly(vinyl alcohol)

PCL	Polycaprolactone
PDI	Polydispersity index
PPDO	Polyparadioxanone
1H NMR	Proton nuclear magnetic resonance
SEM	Scanning electron microscope
$Sn(Oct)_2$	Stannous octoate
SFL	Stop-flow lithography
TEA	Triethylamine
TMC	Trimethylene carbonate
Mw	Weight average molecular weight
XRL	X-ray lithography

CHAPTER 1

INTRODUCTION

The developments in today's pharmaceutical industry have an important place not only in the treatment of diseases, but also in the control of metabolic disorders and the extension of lifespan and quality of life. One of the most important advancements in the pharmaceutical industry is the design of drug delivery systems. The progress in drug delivery systems has made great contributions to the pharmaceutical industry from both economic perspective and patients' point of view. According to the investigations, it costs about $20–50 million to develop brand new drug delivery systems that will make an existing drug more effective, while $500 million is spent to develop a new drug [1]. From the perspective of patients, on the other hand, one of the main purposes of medication is to reduce or remove the effects of disorders and to counter genetic predisposition to certain diseases. The appropriate treatment of metabolic disorders of the body with drugs or surgery not only increase the therapeutic properties of disease, but also improve the lifespan and quality life experience [2]. When taken to the body, the chemical compounds introduced as drugs are first placed in the bloodstream and reach the target tissue through blood vessels. Therefore, the drug is absorbed into cells in all tissues on the vein pathway and processed by cellular mechanisms. In this case, the drug may affect not only the target tissue but also interfere with many unwanted mechanisms in accumulation and metabolism in non-target tissues. In order to increase the delivery of the drug to the target tissue, it is necessary to calculate the drug loss that does not reach the target tissue and to give the drug to the patient at a high dose to compansate this loss [3]. Therefore, the ideal drug delivery system is defined as "getting the

right amount of drug to the right place at the right time." [4], [5], [6]. However, the release of the drug through body may not always be controlled due to the presence of unpredictable parameters [6]. It has therefore become a field that combines science and engineering to design appropriate transport systems that can control the release of drugs and thus improve their therapeutic effects [2], [4].

Innovations in micro- and nanotechnology have accelerated the development of controlled drug delivery systems. The design of portable and implantable devices suitable for drug delivery is directly related to the reduction of the size of the device, and therefore micro-fabricated devices can fill the deficiency in conventional drug delivery systems [7]. Hence, up to now, various microfabrication techniques have been investigated and gathered under two categories: If atoms are tied together to obtain nano and microstructures, it is called bottom-up method. Chemical vapor deposition, sol-gel synthesis and molecular self-assembly are some of the examples for bottom-up processes [8]. On the other hand, if bulk materials are fragmentized to the finer particles, it is called top-down approach. Molding, microfluidic synthesis and photolithography are the most common top-down fabrication techniques [9]. However, with the conventional nano and micro sized particle fabrication techniques, shape control was not adequate which is a substantial parameter in controlled drug release applications since shape of the particle affects carrier transportation and circulation time inside the body [10]. Up to now, several studies have been conducted to emphasize the importance of particle shape especially in drug delivery. Particularly, spherical particles have been compared with disks or elongated particles and it is seen that a macrophage which first met the foreign substance entering the body, internalizes the ellipse particle within a few hours, while the spherical particle internalizes within minutes [10]. Thus, providing definite particle size and shape is critical in drug delivery. DeSimone *et al.* achieved a significant breakthrough in that area by developing the top-down particle replication method, PRINT [11]. Wide range of particulate systems with different shapes and sizes have been produced by means of this

soft-lithography based technique but up to now, poly(ethylene glycol) (PEG), polylactide (PLA) and their copolymers have been utilized for use in drug delivery applications [9], [11]. In fact, polymer-based carriers have outstanding features compared to non-polymeric carriers due to their flexible properties in terms of physical and chemical diversity, so PLA, PEG, poly(glycolic acid) (PGA), poly(lactide-co-glycolide) (PLGA), polycaprolactone (PCL) and their copolymers are broadly used and easily accessible synthetic polymers in drug delivery [12], [13]. Nevertheless, as different type of polymer, recently polycarbonates arouse researchers' interest in biomedical applications [14]. Owing to its superior properties such as slow, unique degradation mechanism and non-acidic, non-toxic products after degradation, poly(trimethylene carbonate) (PTMC) has recently begun to be preferred [14].

In this study, it was aimed to produce PTMC based microparticles which have definite shapes and sizes via soft-lithography molding technique for controlled release applications. Therefore, primarily, high molecular weight PTMC and low molecular weight functionalized PTMC were synthesized. After that, nonwetting fluorinated molds with definite patterns were produced and synthesized material was moulded.

CHAPTER 2

BACKGROUND AND LITERATURE SURVEY

2.1. Controlled Drug Delivery

Controlled drug release has long been one of the most progressive applications in the field of healthcare in which chemists and chemical engineers aim to contribute by working together [15]. They have tried to develop delivery systems that can transport drug to desired part of the body and control the amount of drug released, and these systems are aimed at increasing the effect of active reagent of drug and decreasing toxicity [16]. To achieve this, the concentration of the drug in the plasma must be within the therapeutic range limited by the minimum effective concentration (MEC) and the minimum toxic concentration (MTC) which is called therapeutic window, as shown in Figure 2.1.1. In the conventional delivery systems, generally, when drugs are taken, drug causes to spike in blood concentration and after a while it dramatically decreases under MEC as illustrated in Figure 2.1.1 (solid curve). For this drug to become effective, plasma concentration should be higher than MEC and thus, another dose should be taken. In the course of time, the drug approaches the toxic level MTC (solid curve followed by dotted lines in Figure 2.1.1) and it becomes a poison instead of drug. In order to avoid this toxicity, constant concentration with the appropriate dosage should be given to the patient and plasma concentration lies between therapeutic range as shown in dot-dash line in Figure 2.1.1.

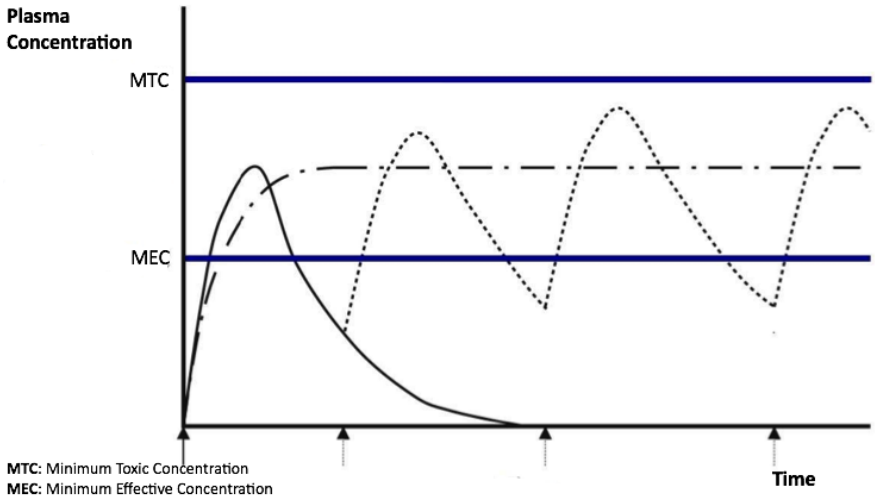

Figure 2.1.1 The plasma concentration profiles in the therapeutic range [17].

In addition to being in the therapeutic window, some of the features that an ideal drug delivery system should possess include biodegradability and biocompatibility, high drug loading capacity, durability and ease of removal of the body [18]. Until now, many drug carrier systems (Figure 2.1.2) have been developed using various methodologies. In a matrix system, the drug carrier has interconnected pores so that the drug follows a tortuous path. A reservoir system, on the other hand, has a semipermeable membrane and the drug passes through this membrane. Degradation and erosion systems show similar release since both release drugs based on degradation. The main difference is in degradable material, pores form during degradation and the drug release is released through these pores, whereas in an erodible carrier, drug dispenses as the substance dissolves. Unlike these, by means of osmotic pressure, drugs release from one pore or many small pores in osmotic pump. Lastly, hydrogels can be used as drug carriers. Thanks to their networked structure, they swell in the solvent medium and release the drug [6].

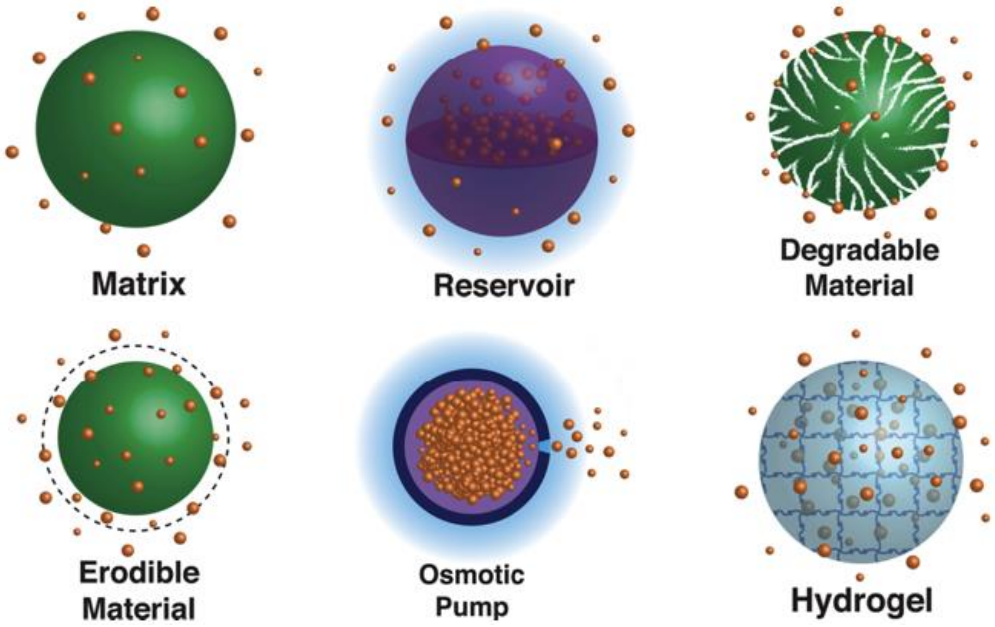

Figure 2.1.2 Controlled release systems developed with various strategies [6].

The development of micro sized carriers to take advantage of controlled drug delivery using these strategies has been preferred particularly in academia and become an outstanding research area.

2.2. Microparticles and Fabrication Methods

Microparticles are preferred in the design of drug delivery systems because they provide the possibility of sustained and controlled in vivo release of the drug, protect in against enzymatic degradation and provide local delivery [19]. Particles with diameters ranging from a few microns are of great interest, such that microspheres 1-5 μm in diameter can be used effectively in the passive targeting of the antigen [20], those 10-20 μm in diameter targeted to the capillary layer of tumor tissues [21], and highly porous particles 5-20 μm in diameter can be used effectively in pulmonary drug delivery [16]. In addition, drug carriers ranging in diameter from 10 to 100 μm are preferred for syringe injections and also not to be transported by the phagocytic cells to the injection site [22]. Due

to its advantages, many commercialized products have been manufactured up to date. Some of these products, which are composed of injectable poly(lactide-co-glycolide) (PLG) based microspheres, are shown as in Table 2.2.1 [23].

Table 2.2.1 Commercially used injectable PLG based microparticles [23]

Trade Name	Treatment
Trelstar®	Prostate cancer
Lupron®	
Sandostatin LAR®	Acromegaly
	Carcinoid syndrome
Risperdal® Consta®	Schizophreni
	Bipolar I
Vivitrol®	Opioid addiction

Although most micro drug carriers that are being developed or approved for use in clinical trials have spherical shape, it appeared that this structure could not be the most suitable form for drug delivery system since aspect ratio and edges have high influences on release kinetics and interactions between cells and particles [10], [24]- [25]. Geng *et al*. for example, have compared the in vivo properties of filamentous micelle structures with spherical ones. According to their study, nonspherical micelles have been found to be able to stay longer in the body compared to the spherical, and the active agent can be more effective when released from filamentous structures. Besides experimental data, the importance of particle shape has also been investigated by theoretical modelling. In the studies, it was proven that spherical and spheroidal particles with 2:1 ratio have different interactions with tumor capillaries. Owing to the external forces, it is difficult to obtain non-spherical polymeric particles. Still, some of the research groups have fabricated such particles by means of different techniques (Figure 2.2.1) [10]. In Figure 2.2.1a, plug shaped microparticle was fabricated via microfluidics. In Figure 2.2.1b, on the other hand, self-assembly method was used to fabricate toroidal poly(styrene) (PS) and in Figure 2.2.1c and d, direct

replication and microscope projection photolithography methods were used, respectively.

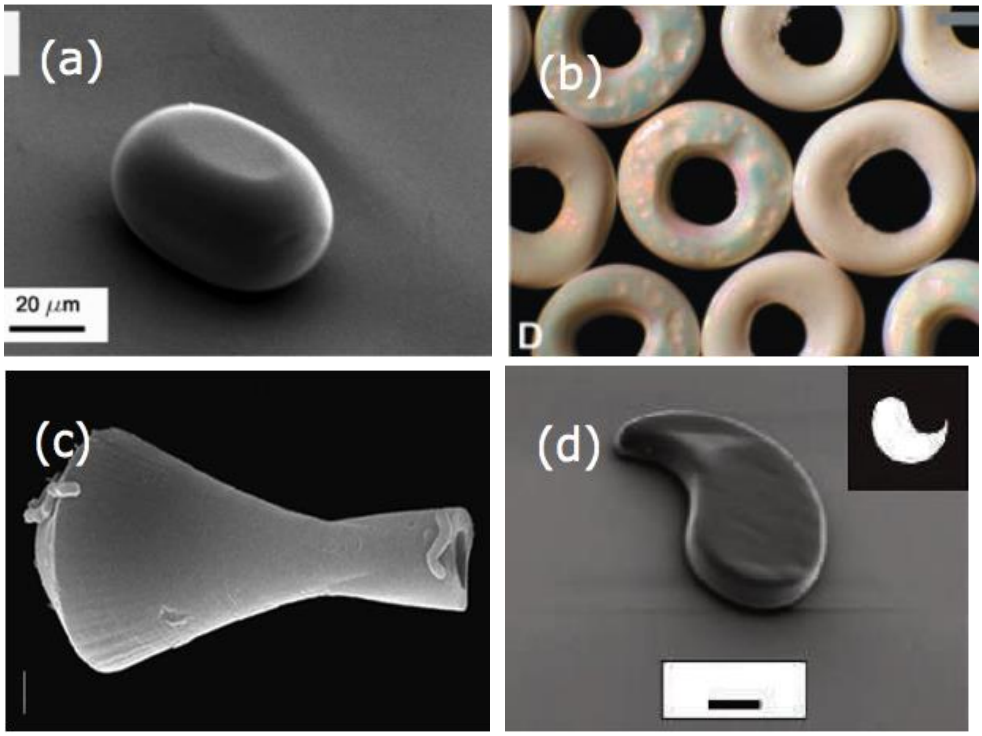

Figure 2.2.1 (a) Plug shaped photopolymer microparticle, (b) toroidal PS microparticles (scale 500 μm), (c) PS vase shaped particle (scale 1 μm), (d) curved PEG microparticle (scale 10 μm) [10].

Different methods have been tried to produce micro and nano sized particles for use in various types of application areas in desired properties and these methods are gathered under two main headings as bottom-up and top-down approach. To begin with the bottom-up method, particles are built up to specifications that are desired starting at the atomic or molecular level. On the other hand, in top-down method, as the name implies, the bulk material is separated into particles at the desired scale (Figure 2.2.2) [9]. In Table 2.2.2, few examples are given related to these fabrication methods [27].

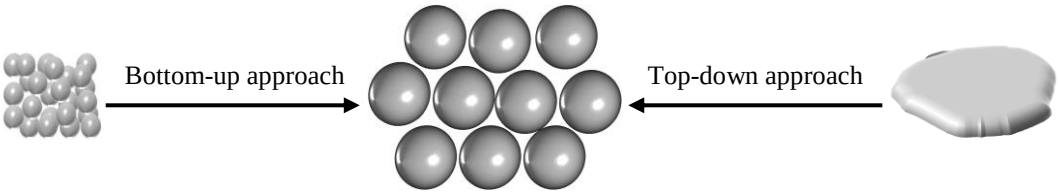

Figure 2.2.2 Schematic illustration of bottom-up and top-down fabrication approaches.

Comparing the suitability of the bottom-up and top-down approaches for developing various drug delivery systems, it can be said that it is very difficult to achieve the control of particle shape in bottom-up methods, which is one of the parameters that greatly affect the interaction between the target tissue and the fabricated material. In this respect, top-down approaches are more precise methods for designing properties such as size and shape, since they are based on tools rather than surface energy and thermodynamics [28]. However, some of the top-down methods may not be suitable for precise shape control and scattered particle size distribution with irregular shapes may be obtained (e.g. grinding, milling). Template and deposition techniques, stretching, microfluidic and photolithographic-like applications are more suitable for creating regular particles.

In hard-template technique (Figure 2.2.3), a conductive sacrificial layer, like gold or silver, is placed on one side of the porous template and the materials of interest are electrochemically filled into these pores. After that, the template is first dissolved to obtain particles on the metal layer. The remaining sacrificial metal layer is also dissolved and particles are obtained. Using this method, generally nanowires, nanotubes and nanorods are prepared [29], [30].

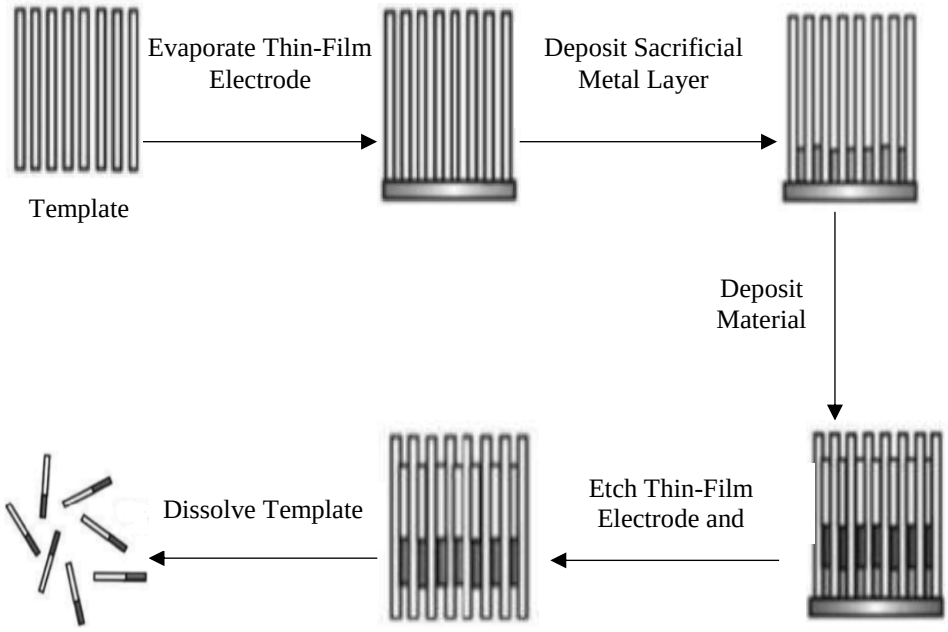

Figure 2.2.3 General illustration of particle fabrication by the hard-template technique [31].

Table 2.2.2 Examples of bottom-up and top-down approaches [27].

Bottom-Up Approach	Top-Down Approach
Gas Phase	**Mechanical Energy**
Chemical vapor deposition (CVD)	Cutting
Atomic layer deposition (ALD)	Rolling
Molecular beam epitaxy (MBE)	Milling
	Grinding
	Stretching
Liquid Phase	
Molecular self-assembly	**Thermal**
Supramolecular chemistry	Electrospinning
Nucleation	Extrusion
Sol-gel process	
Single crystal growth	**Chemical**
Electrodeposition	Chemical etching
	Anodizing
	Lithographic
	Photolithography
	X-ray lithography (XRL)
	Electron beam lithography (EBL)
	Microcontact printing methods
	Nanoimprint lithography (NIL)
	Natural
	Erosion
	Hydrolysis

In the mechanical stretching technique (Figure 2.2.4), mainly, PS particles are embedded in PVA film. The PS is permitted to flow by bringing it to the deformation temperature or by adding solvent. Different particle shapes are obtained from the PS which fills the gaps in the film or deforms by hydrogen bond attraction. Although twenty types of particle shape are formed by changing the parameters such as reducing the temperature of solvent etc., the biggest handicap of this method is that material compatibility cannot be achieved and therefore it is not suitable for the material diversity [32], [33].

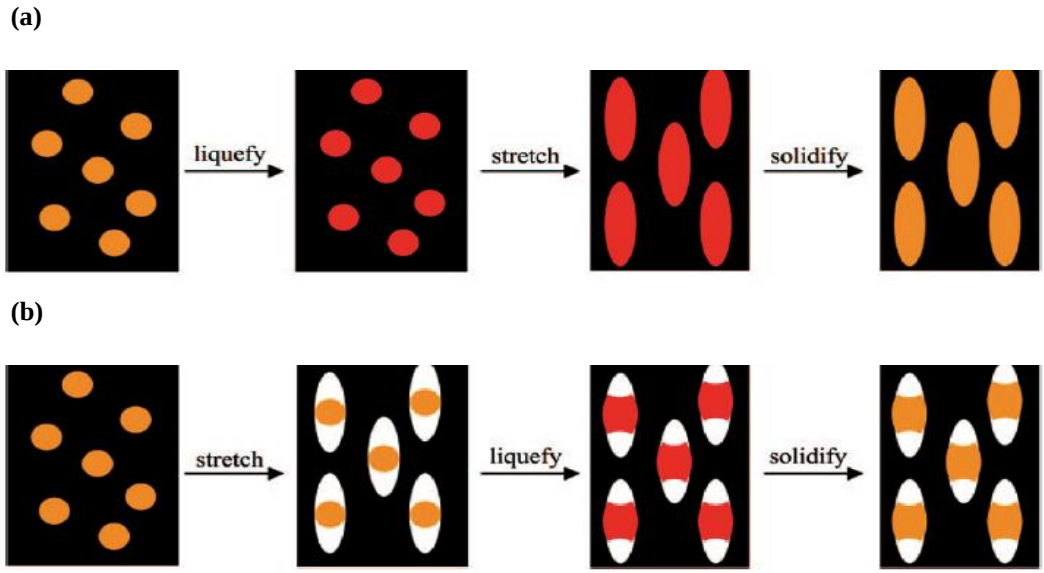

Figure 2.2.4 Schematic illustration of particle fabrication by general stretching methods. a) First, particles are liquefied via heat or solvent and then solidified by evaporation of solvent or cooling. b) First the film is stretched in air to create voids [34].

Microfluidic devices (Figure 2.2.5) are one of the systems developed to be able to provide control over particle shape and size components, which are limited to be able to form sphere and cylinder-like particles [35]. More complex structures were produced by changing the geometry of the device, the fluid flows and also by using photolithography mask [36]. In photolithographic systems, usually the particles are cross-linked by rapid exposure to UV light rapidly [37]. In addition, systems in which the monomer flow is stopped for a short time during each exposure to obtain a higher resolution are also referred to as stop-flow lithography (SFL), and much more complex structures can be produced by this system [36], [38]. Although various particle shapes such as pyramids, rectangles, spheres, and rectangular toroids, etc. can be designed in a controlled way, the major disadvantage of microfluidic systems is that they can not only allow material diversity because they need to be worked only with polymerizable fluids [39].

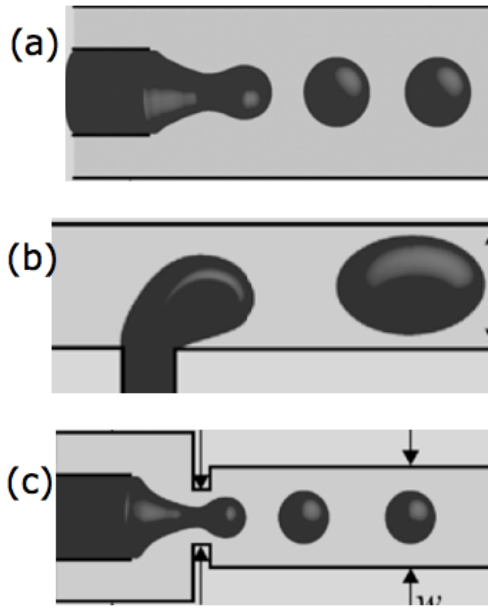

Figure 2.2.5 Display of three different microfluidic device geometries [40].

Another alternative to generate monodispersed particles is photolithography based techniques. The suitability for mass production is also the reason for preference [41], [42]. By using photolithographic techniques, particles' surface roughness [43], shape diversity [44], adaptability to different materials such as organic dyes and iron oxide particles [44] have been studied even in nanometer scales. One of the attractive features of this method is to obtain exactly the expected particle shape. Nonetheless, continuous lithographic exposure process is a financial burden and there may not always be found suitable conditions for this process [45]. Therefore, the idea of developing templates which can be used repeatedly have been introduced [46]. According to the study conducted by Xia *et al.* in 1998, primarily, original rigid template which includes patterns was conceived through conventional photolithographic techniques. Afterwards, by way of original template, elastomeric replica molds were produced to use in molding and stamping and this technique is called soft-lithography. At the beginning of the development of soft-lithography technique, it was strenuous to form free particles since after the interested material was molded on crosslinked

poly(dimethylsiloxane) (PDMS) elastomeric mold, eventual particles were linked to each other. In other words, there was a residue layer so-called flash layer [47]. Many studies have been investigated to remove the flash layer and obtain free particles directly such as oxygen plasma etching or dissolution the residue layer [48]. Both were observed to have an extra step, cause time loss and lead to hassle. Surface modifications of the PDMS mold have been tried, such as increasing or decreasing the hydrophilic nature of the surface. One of the breakthrough innovations in this sense has been the development of Particle Replication in Non-wetting Templates, namely PRINT® technology. As seen in Figure 2.2.6, fluorinated elastomeric mold is used in this technology, which differs from traditional lithographic techniques in that it provides a non-wetted surface that facilitates the filling of the mold and particle release [9], [11], [25].

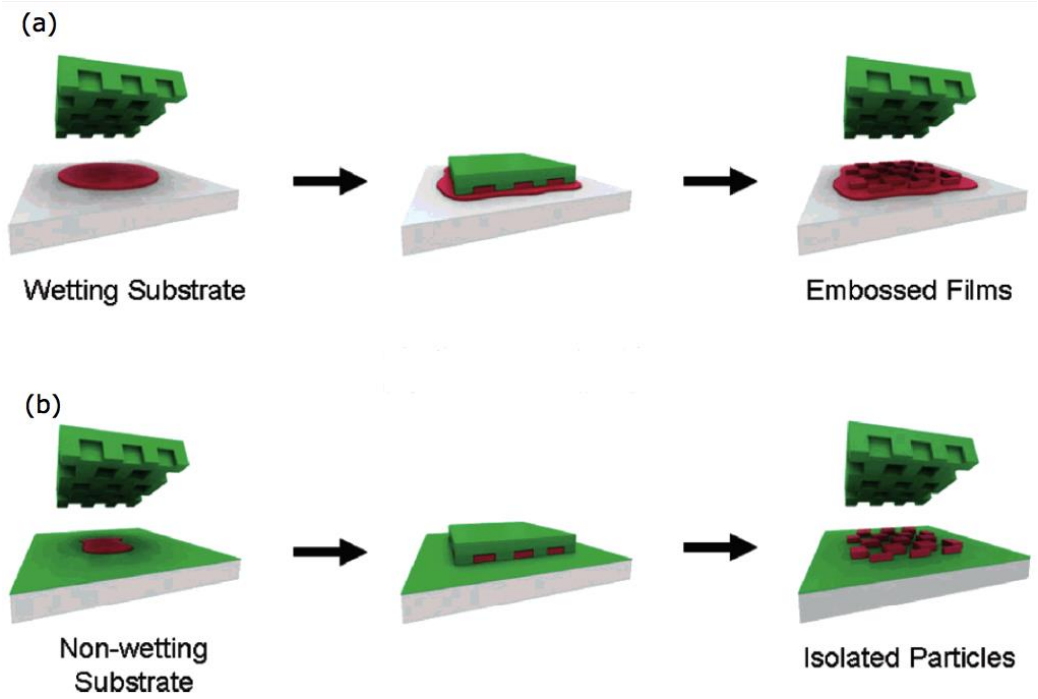

Figure 2.2.6 A schematic illustration of the comparison of a) traditional lithographic technique, b) PRINT process. Green is fluorinated mold and red is pre-particle solution [11].

2.3. Overview of Particle Replication in Non-Wetting Templates (PRINT) Technology

In soft-lithography based techniques, mostly PDMS has been preferred due to the plethora of advantages such as;

- elastomeric material with low Young's modulus (~750 kPa),
- smoothly released from the patterned mold due to the low surface energy (~20 erg/cm^2),
- allowing gas permeability,
- nontoxic nature [49].

Despite its spectacular advantages, PDMS poses a huge problem by swelling in commonly used organic solvents like hexane, toluene, acetone, dichloromethane, acetonitrile, and ethyl ether. Since this feature restricted the use of PDMS, a new system to be used in the soft lithography technique had to be developed. Perfluoropolyether (PFPE) based elastomer synthesis was considered to be suitable for such an application. Synthesis and curing procedure is summarizeed in Figure 2.3.1.

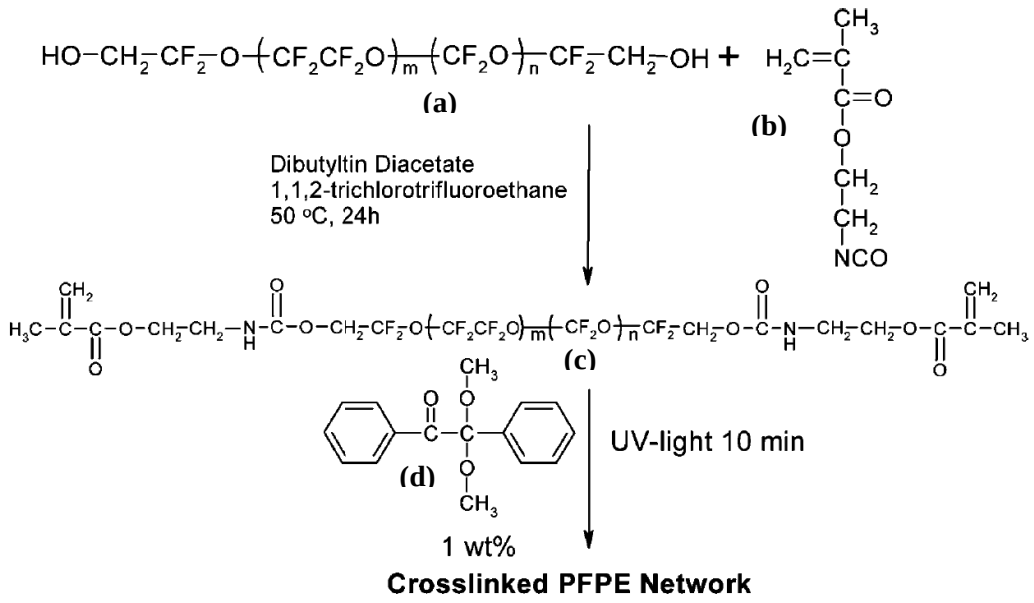

Figure 2.3.1 Schematic presentation of chemical structure and synthesis of photocurable PFPE. Briefly, fluorinated PFPE diol (a) was functionalized with isocyanatoethyl methacrylate (b) to form PFPE dimethacrylate (c). With the addition of photoinitiator (d), crosslinked PFPE network was obtained by exposed to UV light (365 nm, ~10-15,000 mJ/cm^2) [49]

Comparing the obtained PFPE elastomers with PDMS templates used in soft lithography, it can be seen that using fluoro-based elastomer has significant advantages like;

- easily removable flash layer due to its low surface of energy (~8-10 erg/cm2) [50],
- no requirement for an additional step such as etching or plasma [46], [51],
- compatibility with organic solvents particularly that PDMS is not suitable (Table 2.3.1) [52],
- more accurate replications were obtained from the master and it was possible to reproduce smaller feature sizes [50].

Table 2.3.1 Swelling behavior comparison of PDMS and PFPE [52].

	PDMS (weight % uptake)	PFPE (weight % uptake)
Water	0.37 ± 0.04	0.39 ± 0.16
Hexane	109.82 ± 1.41	1.72 ± 0.25
Tetrahydrofuran	145.46 ± 1.68	6.95 ± 0.08
Dimethyl sulfoxide	2.36 ± 0.50	1.98 ± 0.17
Isopropanol	17.65 ± 2.44	2.38 ± 0.06
Acetone	20.15 ± 1.05	4.81 ± 0.06

The PRINT technique has emerged with the discovery of the superior properties of PFPE and its adaptation to the soft-lithography applications. To summarize this technique, firstly, patterned silicon wafer used as master is fabricated by standard photolithographic techniques (Figure 2.3.2). In this technique, UV light is sent through a mask having a desired pattern to silicon wafer coated with a thin film layer of photosensitive resist and the pattern is obtained either by dissolving or crosslinking [53]. Thereafter, as shown in Figure 2.3.3, elastomeric mold is prepared by casting and curing PFPE precursor onto the master mold. Now, as the patterned PFPE mold is prepared, the liquid pre-material can be filled into the elastomeric mold's cavities by capillary forces. Since PFPE has Teflon-like property, there would not be any liquid material on the mold's surface, in other words, material fills into the wells without wetting the surface area. Liquid is solidified to take the shape of the wells and the particles are removed from the mold by getting in touch with a harvesting layer. The particles can now be easily harvested from the surface of the flat layer [9].

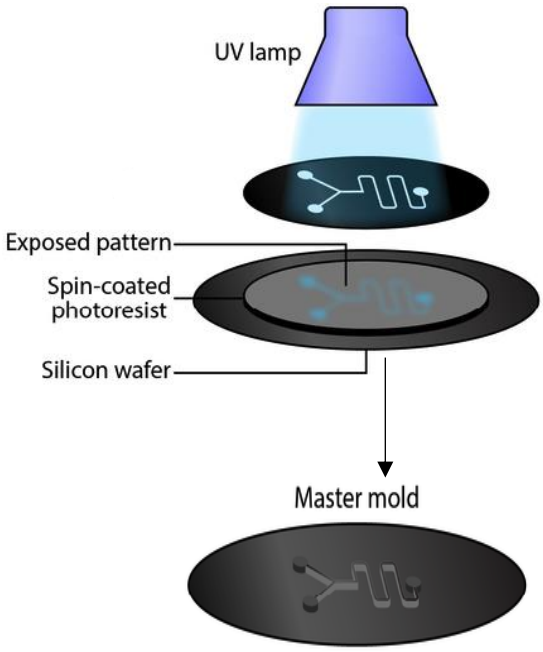

Figure 2.3.2 Standard photolithography technique [54].

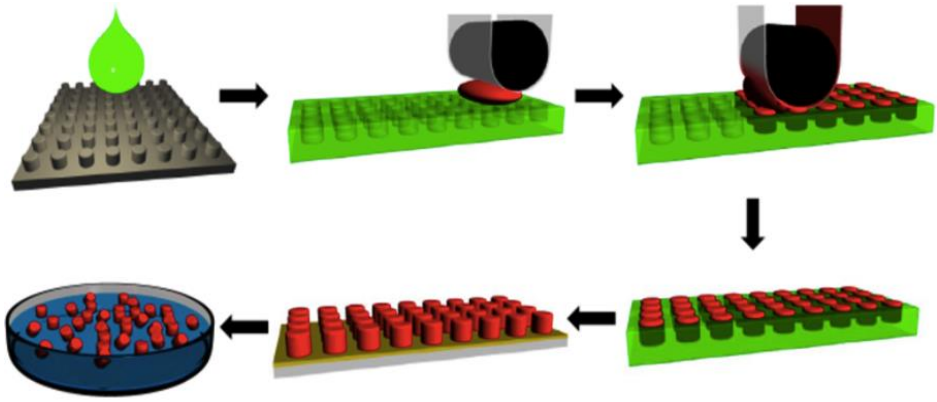

Figure 2.3.3 Schematic illustration of PRINT process [9]. (Gray is rigid silicon wafer, green is PFPE elastomeric mold, red is pre-particle substance, black is roller, yellow is harvesting film.)

Until now, many articles have been published regarding PRINT technique varying in both sizes and shapes. Rolland and colleagues in 2005 fabricated 200 nm trapezoidal poly(D-lactic acid) (PLA) and derivatives poly(lactide-co-glycolide) (PLGA) (Figure 2.3.4 a), submicron (500 nm) conical PLA (Figure 2.3.4 b), 200 nm trapezoid poly(pyrrole) (PPy) (Figure 2.3.4 c), 200 nm trapezoidal, 200 nm x 800 nm bar, 3 μm arrow PEG-diacrylate liquid monomer (Figure 2.3.4 d, e, f and g, respectively) and 200 nm trapezoidal triacrylate particles (Figure 2.3.4 h).

Gratton *et al.* in 2008 prepared cubic and cylindrical particles with the composition of 67 wt % trimethyloyl propane ethoxylate triacrylate, 20 wt % poly(ethylene glycol) monomethylether monomethacrylate, 10 wt % 2-aminoethylmethacrylate hydrochloride, 2 wt % fluorescein o-acrylate, and 1 wt % 2,2-diethoxyacetophenone. Scanning electron microscope (SEM) and fluorescence images of the fabricated particles are given in Figure 2.3.5 [25]. In another manuscript, 3 μm PEG based hex nut shape particles were also published (Figure 2.3.6).

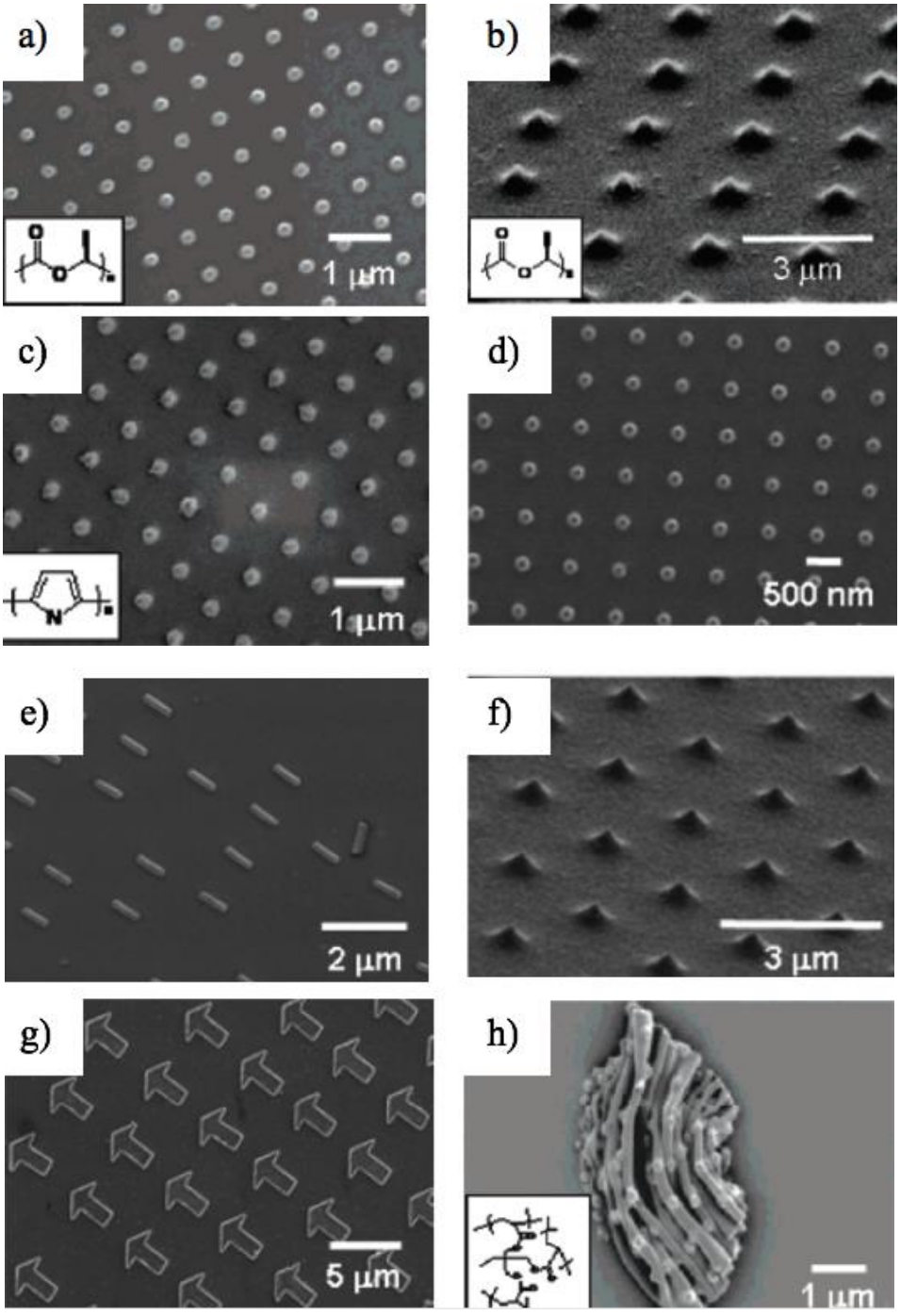

Figure 2.3.4 SEM images of fabricated PLA, PPy and PEG based particles via PRINT technique [11].

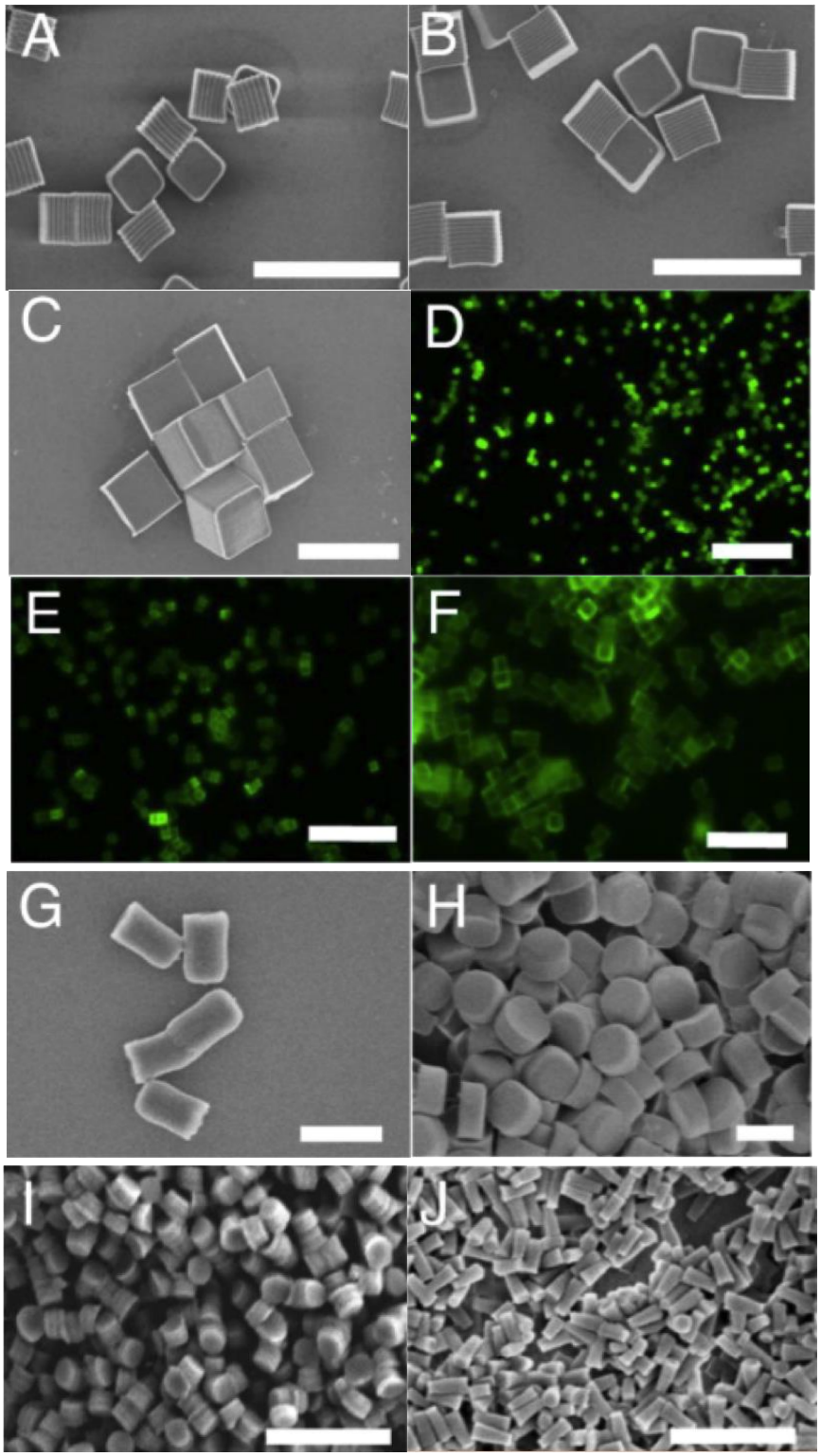

Figure 2.3.5 (A-C) SEM images of the cubic particles with diameters equal to A) 2 μm, B) 3 μm and C) 5 μm. (D–F) Fluorescence images of the cubic particles

with diameters equal to D) 2 μm, E) 3 μm, and F) 5 μm. (G-H) SEM images of the cylindrical particles having the height of 1 μm, and G) 0.5 μm, H) 1 μm diameters. (I–K) SEM images of the cylindrical nanoparticles with I) 200 nm diameter, 200 nm height; J) 100 nm diameter, 300 nm height [25].

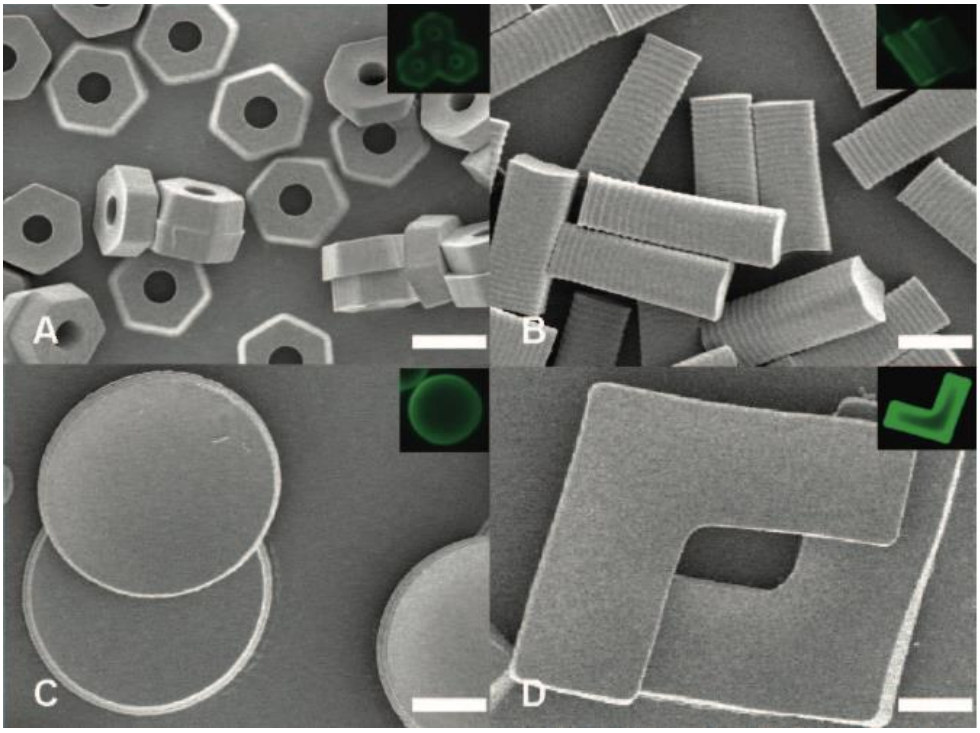

Figure 2.3.6 SEM and fluorescence images of (A) 2.5 × 1 μm^2 hexnut particles with a 1 μm hole, (B) 1.6 × 1.6 × 5 μm^3 trapezoidal particles, (C) 6.5 × 0.8 μm^2 disk shaped particles, and (D) 9.6 × 3.4 × 1 μm^3 boomerang shaped particles [56].

Although there are many publications so far, only a few types of polymeric material have been used to fabricate micro and nano scale drug delivery devices via PRINT technology.

2.4. Synthetic Biodegradable Photocrosslinked Polymer Networks

Erosion and degradation of polymers are crucial especially for designing injectable or implantable treatment systems in tissue engineering applications [17], [57], [58]. In cases where the implanted material is desired to be permanent, non-degradable polymers are suitable materials [59]. However, in many applications it is desired that the polymer entering the body should be biodegradable. Hydrolysis, oxidation [60], thermal degradation [61] and radiolysis [62] can cause polymer degradation. In order to be a biodegradable polymer, hydrolysable bonds (esters, anhydrides, urethanes, amides, carbonates, etc.) must be present in the structure because chain cleavage is denominated as degradation [57], [63]. On the other hand, dissolution and diffusion of monomers or oligomers cause the material loss so called polymer erosion which is divided as surface and bulk erosion (Figure 2.4.1). Basically, in surface erosion, as the name implies, polymers only lose material from the surface. Thereby, dimensions and mass of the polymers decreases proportionally, whereas molecular weight remains constant. In bulk erosion, the mass and dimensions of the polymers are unchanged while molecular weight decreases and consequently, mechanical properties change during the application [57]- [58], [64]- [65].

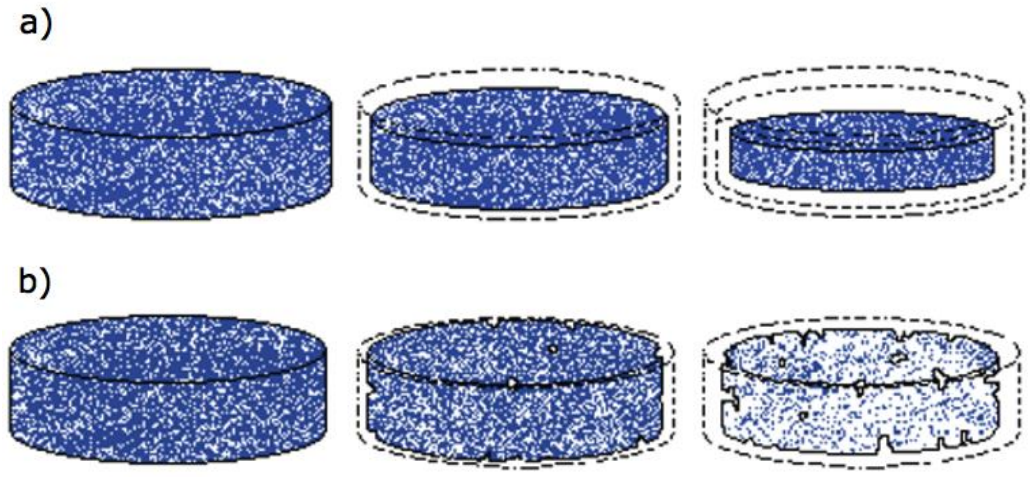

Figure 2.4.1 Schematic representation of a) surface, and b) bulk erosion process [65].

While designing a new polymeric material for drug delivery applications, biodegradable photo-crosslinked networks come to the forefront since desired amount of drug can be loaded handily and efficiently into the polymer matrix (Figure 2.4.2) and release profile of drug can be varied by changing crosslink density and hydrophilic/hydrophobic properties of the network [66].

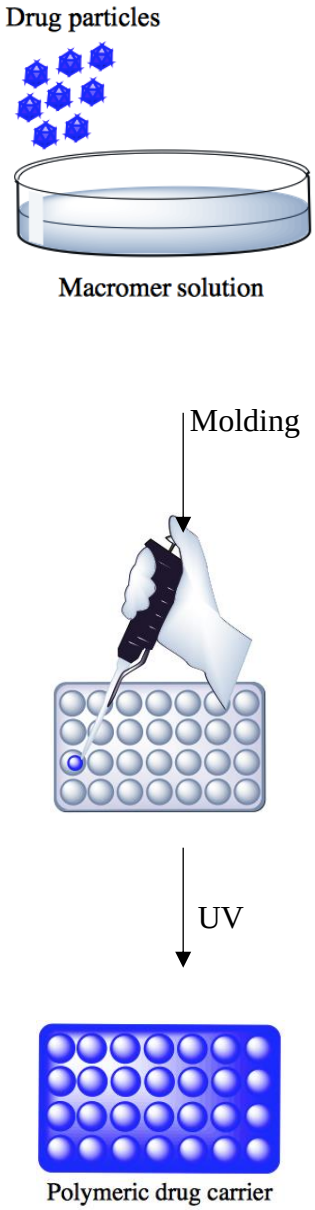

Figure 2.4.2 General diagram of photo-crosslinked polymer network preparation. Macromer solution is prepared and drug particles are mixed with

the solution. The viscous material is poured onto the mold and after photo-crosslinking, solid drug carrier is ready.

Polymeric networks are macromolecules formed by permanent attachment of unit or monomer to the other unit. This network formation can be derived from the formation of covalent or ionic bonding, or physical interactions. Among them, covalently crosslinked networks are widely preferred due to the enhanced properties such as improved strength, flexibility, and durability. Covalent crosslinks can be formed by chemical reactions initiated by heat, pressure, pH change or light irradiation [67]. Photo-initiated crosslinking (Figure 2.4.3) is used for a number of applications compared to other methods because of its properties such as low energy and space requirement, high speed at room temperature, environmental advantages, etc. [68]. Basically, after the polymerization is initiated by light, a photo-initiator disintegrates and generally forms two radicals. These radicals react with -C=C- bonds of macromer to form a growing kinetic chain. In order to prepare biodegradable photo-crosslinked polymer networks, end functionalized degradable oligomers are often used with groups containing double bonds i.e., fumarate, acrylate, and methacrylate, end groups (Figure 2.4.4) [69]. Fumaric acid derivatives are attractive compounds for end-functionalization since they take place in the citric acid cycle in the body, that is, they are not expected to cause to toxicity [70]. However, the reactivity of the fumarate-functionalized oligomers is relatively low compared to oligomers that are functionalized with acrylate and methacrylate [71]. Thus, methacrylate and acrylate derivatives are frequently used in end-functionalization reactions.

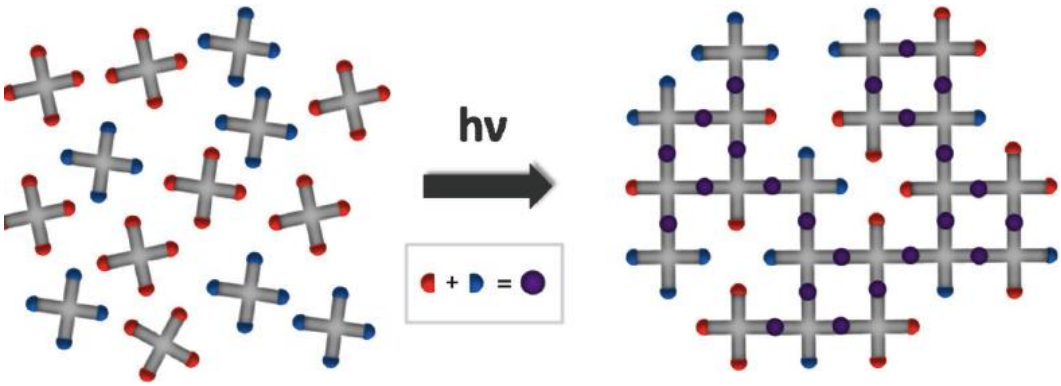

Figure 2.4.3 Schematic representation of photo-crosslinked network formation [67].

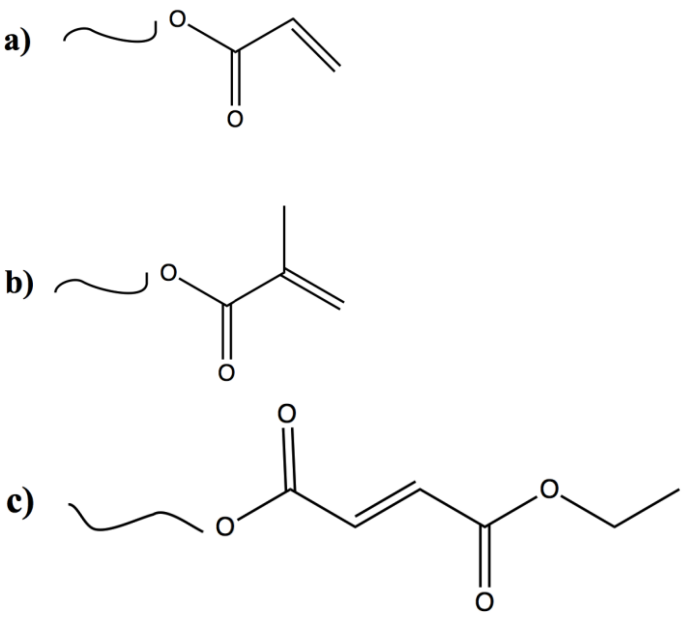

Figure 2.4.4 Photopolymerizable a) acrylate, b) methacrylate, and c) fumarate end groups.

In light of all these information, it can be said that studies on drug delivery systems with the help of synthetic biodegradable polymers have taken place in the literature, though not yet sold on the market. More broadly, it can be seen that various biodegradable polymers are used in many tissue engineering fields, not just drug delivery systems. To exemplify, polyesters such as

polyparadioxanone (PPDO), PLA, polyglycolic acid (PGA) and their copolymers have been improved to be used in bone repair and drug releasing systems [72]- [73]. Degradation of the polyester inside the body is the bulk eroding process. By hydrolysis, the polymer is converted into lactic acid and glycolic acid monomers. The resulting lactic and glycolic acids disrupt the pH balance, causing inflammatory foreign body response and bone resorption [74], [75], [76]. Unlike the bulk erosion mechanism of synthetic polymers, the release rate can be adjusted successfully using surface erosion mechanism. In this sense, polycarbonates are prominent biodegradable materials and PTMC is one of the best examples [14], [77]- [78].

PTMC was originally synthesized and published in 1930 but has not been used in medical fields until 1970s [79]. It is synthesized by ring opening polymerization of trimethylene carbonate (TMC) monomer (Figure 2.4.5) [80]- [81]. PTMC is a hydrophobic, non-crystalline, in other words, amorphous polymer with a glass transition temperature (T_g) of -17 ^oC [82]- [83]. Due to its hydrophobicity, it can be used as hydrophobic part of amphiphilic copolymers and due to its flexibility, it is preferred in soft tissue engineering applications. Flexible structure can be advantageous as well as disadvantageous. Since there is no cross-linking, PTMC may not be able to maintain a stable form, which is unfavorable for controlled drug release because alteration of surface area and shape means a change in the properties of the designed drug carrier [84], [85]- [86]. PTMC is also durable to in vitro non-enzymatic hydrolysis [77], [84], [83], [87] and in vivo enzymatic surface erosion mechanism makes PTMC as an attractive material in biomedical applications [77], [88]. After degradation of PTMC with lipase enzyme, non-acidic products such as 1,3-propanediol, TMC monomers and oligomers are formed [77].

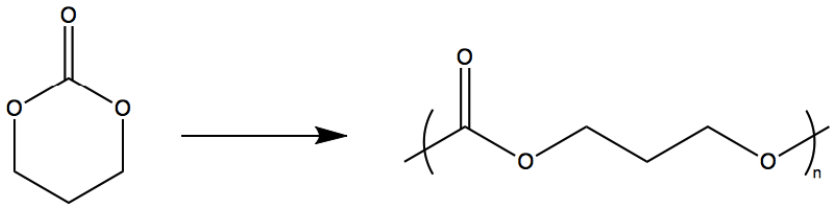

Figure 2.4.5 Ring opening polymerization of TMC monomer.

Several studies have been conducted until now to apply TMC-based polymers in developing drug delivery systems to utilize superior degradation properties compared to commonly used polymers (Table 2.4.1)

Table 2.4.1 Literature summary of PTMC based particles used in biomedical applications. (PGlu: Poly(glutamic acid); Pep: Peptide)

Material	Fabrication Method	Reference
PTMC-b-PGlu	Self-assembly	[89], [90]
PTMC-b-Pep-b-PGA	Self-assembly	[91]
PEG-co-PTMC	Self-assembly	[92], [93], [94], [95], [96], [97]
Pep-b-PEG-b-PTMC	Self-assembly	[98]
PEG-PTMC PEG-PLA/PTMC	Photo-polymerization	[99]

CHAPTER 3

MATERIALS AND METHODS

3.1. Materials

Trimethylene carbonate (1,3-dioxan-2-one, TMC) was used as received from Huizhou Foryou Medical Devices Co., China. Methacryloyl chloride (MC) was purchased form Alfa Aesar. Trimethylol propane and 1-hydroxycyclohexyl phenyl ketone photoinitiator were supplied from Tokyo Chemical Industry Co., Ltd. (TCI). Stannous octoate (tin 2-ethylhexanoate, $Sn(Oct)_2$), 1H,1H,2H,2H-perfluorodecyltriethoxysilane (PFDTS) and 3-(trichlorosilyl)propyl methacrylate were obtained from Sigma Aldrich. Sylgard 184 silicon elastomer kit were supplied from Dow Corning. Perfluoropolyether (PFPE) urethane methacrylate (MD700) was supplied from Acota Limited (UK). Hydroquinone, triethylamine (TEA) and all solvents were used as received from Sigma-Aldrich. Chromafil® Xtra Polytetrafluorethylene-45/25 syringe filters were supplied from Macherey-Nagel. Silicon patterned wafers (< 100 μm) were provided by METU-MEMS Center.

3.2. Preparation of High Molecular Weight PTMC, Functionalized PTMC as Crosslinking Agent and PTMC Film

High molecular weight PTMC was synthesized by ring opening polymerization of TMC monomer using 0.02 mol % $Sn(Oct)_2$ catalysis at 130 ^oC under nitrogen for 3 days. Three-armed PTMC oligomers (Figure 3.2.1) were synthesized by using trimethylol propane (11 mol %) initiators, respectively in the presence of $Sn(Oct)_2$ (0.02 mol %) catalyst under nitrogen at 130 ^oC for 48 h. To obtain functionalized hydroxyl end groups, firstly, oligomers were dissolved in dichloromethane (DCM). 30 mol % excess MC were reacted with oligomers in the presence of 0.06 wt % hydroquinone and excess amount of TEA at 0 ^oC overnight. The functionalized PTMC macromers were further purified by dissolution in acetone and precipitation into water. After freeze drying, degree of functionalization of three-armed crosslinking agents (Figure 3.2.2) were analyzed by ^1H NMR analysis.

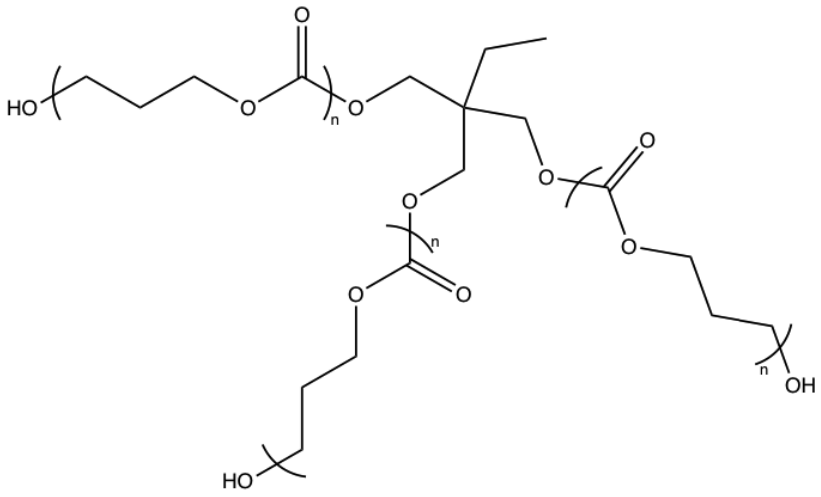

Figure 3.2.1 Chemical structures of three-armed PTMC oligomers

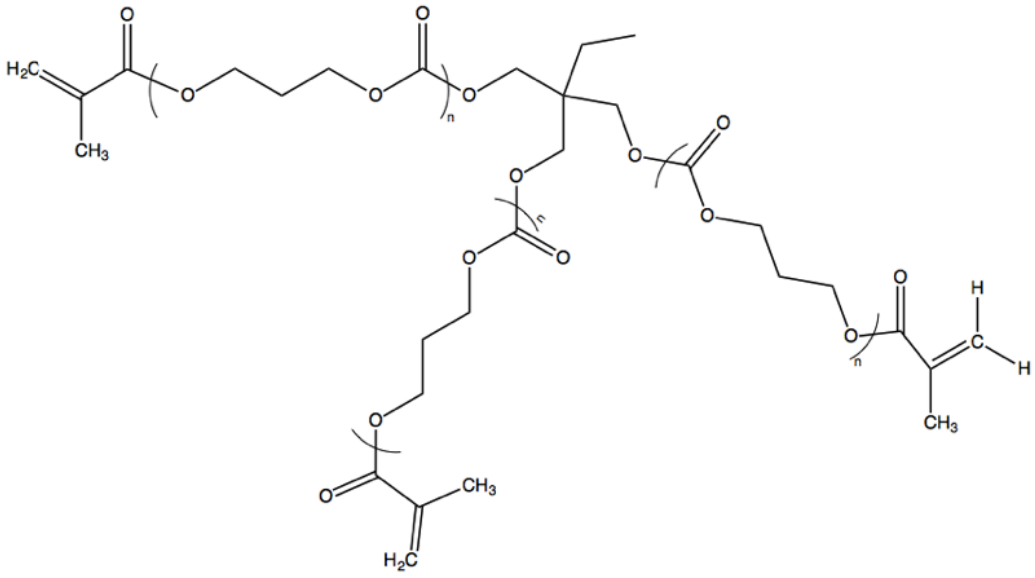

Figure 3.2.2 Chemical structure of functionalized three-armed crosslinking agents

3.3. Fabrication Procedure of PTMC Based Microparticles

3.3.1. Mold Fabrication

Silicon master with desired indentations was produced by standard lithographic techniques. To generate elastomeric polydimethylsiloxane (PDMS) stamps, silicon master was cleaned with 10-min O_2 plasma (Diener Electronic, Zepto Plasma Unit) and exposed to PFDTS vapor in a vacuum desiccator for approximately 9 hours. Silicon elastomer was mixed with curing agent in a ratio of 10:1. After chemical vapor deposition of silane on patterned master, PDMS was poured over the master and cured at 80 ^{o}C overnight. PDMS mold with inverse pattern was stripped from the master and exposed to PFDTS vapor in a vacuum desiccator for 9 hours. In a similar manner, flat PDMS was prepared and coated with silane to attain non-wetting surfaces (Figure 3.3.1).

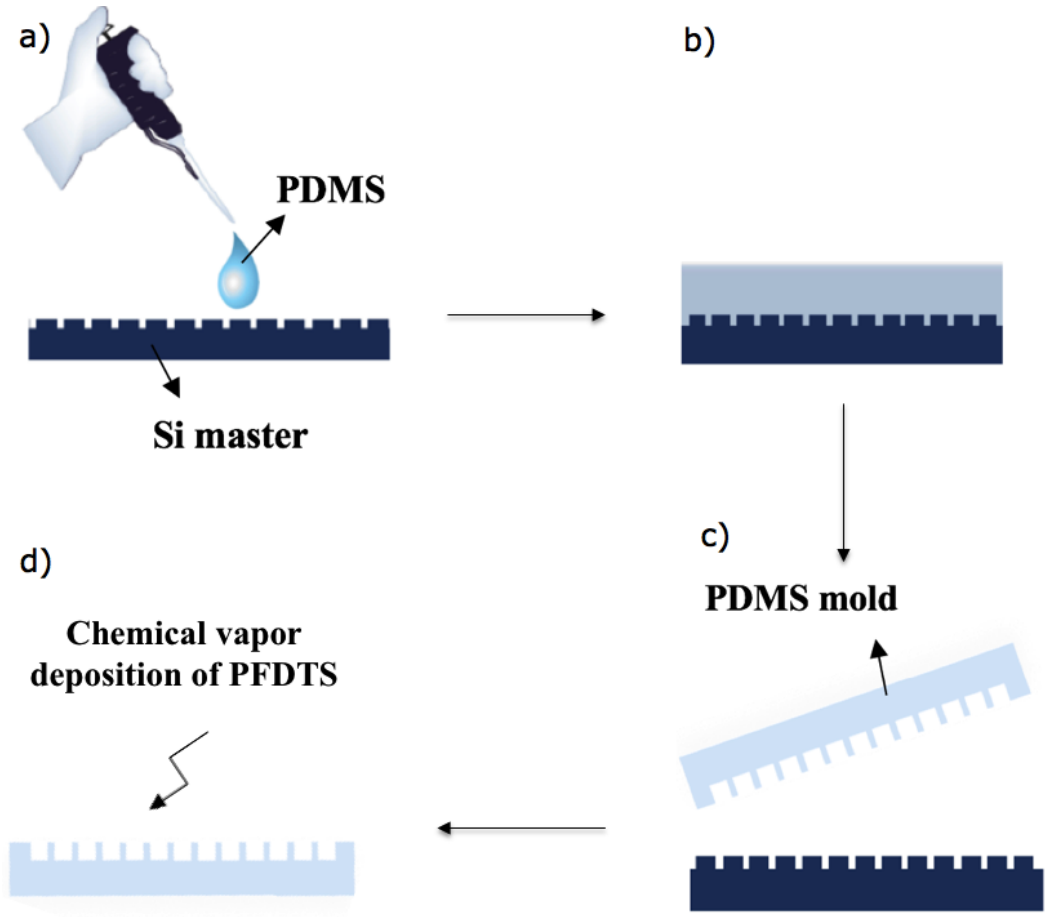

Figure 3.3.1 Non-wetting PDMS based mold fabrication process. a) PDMS was poured onto Si master, b) having wetted the template surface, PDMS was cured, c) Inverse pattern was obtained by peeling fabricated mold from the template, d) patterned surface was exposed to PFDTS vapor.

Besides PDMS stamps, PFPE mold with glass slide backing was produced. Vapor of 3-(trichlorosilyl)propyl methacrylate on microscope slide was deposited in vacuum desiccator as described above. PFPE was mixed with soluble 1-hydroxycyclohexyl phenyl ketone photoinitiator in the ratio of 100:1 and a drop of solution was poured onto silicon master. The master was contacted with microscope slide and exposed to UV light for 30 min.

To obtain non-wetting, non-reactive fluoropolymer mold, nitrogen was bubbled through PFPE solution for approximately 2 minutes. After the displacement of oxygen with nitrogen, the solution was placed under vacuum for 5 minutes to remove all the bubbles. Prepared PFPE solution was poured onto silicon wafer patterned by standard lithographic techniques and cover the surface of it (Figure 3.3.2a). After the pattern was completely wetted, PFPE was exposed to UV light for 30 min under nitrogen purge (Figure 3.3.2b). The crosslinked PFPE was stripped from the wafer and inverse patterned non-wetting mold was obtained (Figure 3.3.2c). In a similar manner, flat PFPE surface was created by pouring PFPE solution onto a flat wafer.

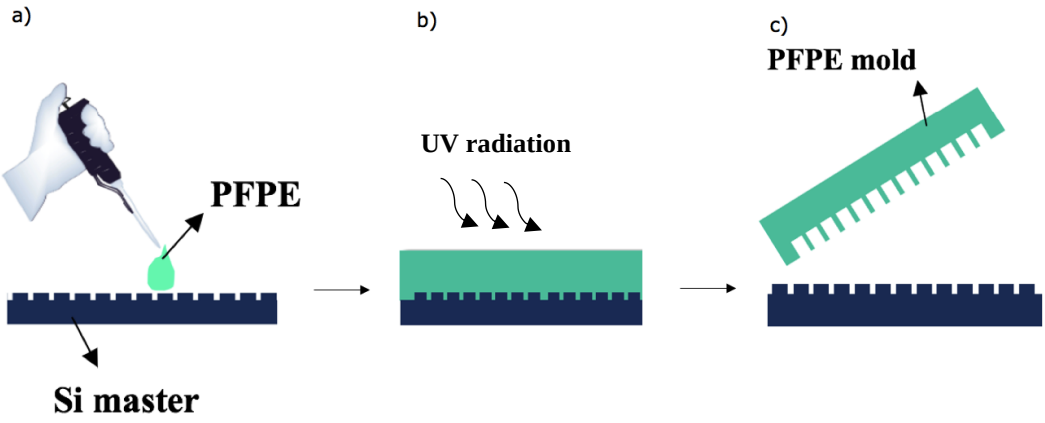

Figure 3.3.2 PFPE based mold fabrication process. a) PFPE was poured onto wafer, b) having wetted the template surface, PFPE was exposed to UV light, c) Inverse pattern was obtained by peeling fabricated mold from the template.

3.3.2. High Molecular Weight PTMC Based Microparticle Fabrication

Since it was desirable for the particles to have cross-linked architecture, high molecular weight PTMC (98 mol%), tri-functional PTMC oligomers (2 mol%) and photoinitiator were dissolved in chloroform. After obtaining homogenous mixture, it was poured into a petri dish and dried under vacuum. The sample was then pressed in compression molding at 140 ^{o}C, 1 atm and filmed. The film was placed between flat and patterned PFPE molds and put on the NIL device (CNI v2.0 – Desktop nanoimprint tool), as shown in Figure 3.3.3. The imprint

temperature was increased to 140 °C, allowed to stand for 5 minutes under 5 bar pressure and then exposed to UV light for 30 minutes under the same conditions. After curing was complete, pressure and temperature brought into ambient conditions.

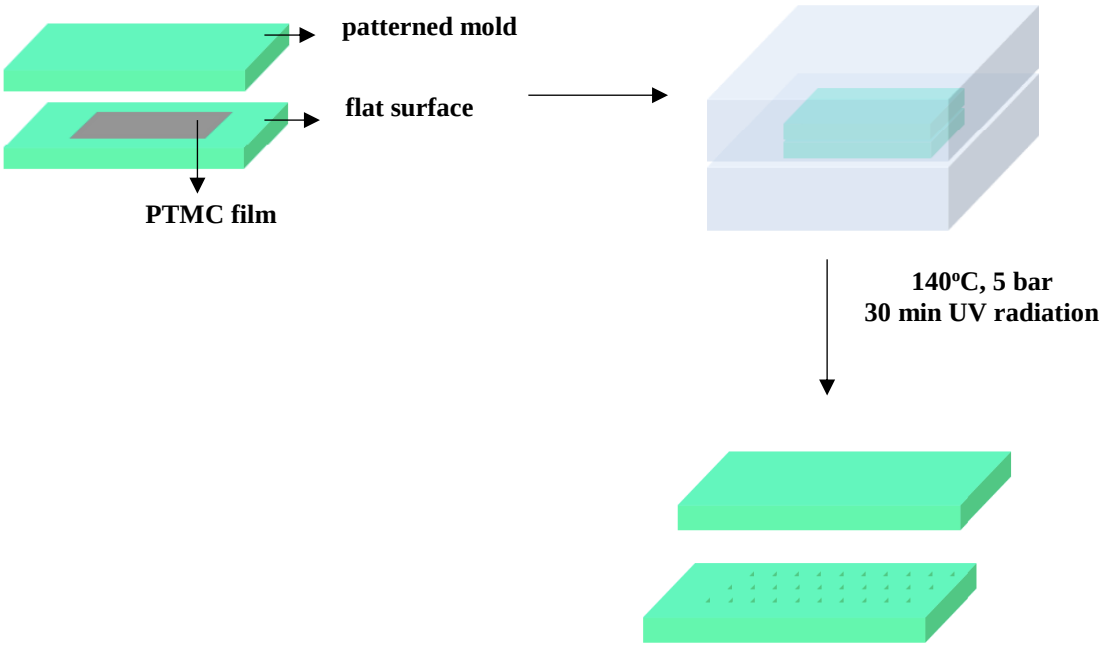

Figure 3.3.3 Schematic representation of high molecular weight PTMC based micro particles fabrication procedure. The film was placed between flat surface and patterned mold, the structure was put onto the NIL device, after curing the mold and the surface were separated.

3.3.3. Low Molecular Weight PTMC Based Microparticle Fabrication

Multiple mold filling methods were applied to prevent the formation of the scum layer. In all the methods, functionalized three-armed PTMC oligomer and hydroxycyclohexyl phenyl ketone photoinitiator were used as the resin in a weight ratio of 100:1. The resin was then dissolved in chloroform and 5 % (w/v) pre-particle solution was obtained.

3.3.3.1. PTMC Based Microparticle Fabrication by Nanoimprint Lithography

In a similar manner shown in Figure 3.3.3, PTMC resin was casted between flat and patterned PDMS surfaces. Flat-PDMS/PTMC/patterned-PDMS sandwich structure was then placed in NIL device. After applying 5 bar for 5 minutes at ambient temperature, the sandwich structure was exposed to UV light for 30 minutes under nitrogen purge. Same procedure was repeated with flat-PFPE/PTMC/patterned-PFPE with glass slide backing and flat-PFPE/PTMC/patterned-PFPE sandwich structures.

3.3.3.2. PTMC Based Microparticle Fabrication by Coating Patterned Mold

Cavities on PFPE mold were filled using SPS Spin 150 coater. 5 % (w/v) pre-particle solution was dropped onto the mold and spin coated at 3000 rpm for 10 minutes. Then, the mold was put under vacuum for approximately 20 minutes to evaporate all residual solvent. Removing the solvent, the resin was exposed to UV radiation for 30 minutes under nitrogen purge and allowed to take shape of the patterns by crosslinking.

Another approach was coating PFPE mold using #1 Mayer rod which is known as a wire-wound rod. Simply, stainless steel is wound with again stainless steel wires in different diameters as shown in Figure 3.3.4 [100] - [101] and it can be used in numerous coating applications [102] - [103]. Outer diameter of the rod is 3 mm and wire diameter is 50 μm for #1 Mayer rod. Here, PTMC resin was spread over PFPE mold by the help of Mayer rod and after filling the cavities, the mold was exposed to UV light for 30 minutes under nitrogen purge.

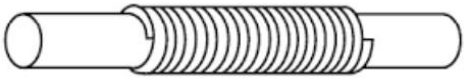

Figure 3.3.4 Drawing of a Mayer rod or wound-wire rod [100]

3.3.4. Particle Harvesting

Particle harvesting was the final step of particle fabrication. Here, three different methods have been tried to collect particles properly. Initially, PTMC film was placed in contact with PTMC oligomers filling the pattern of the mold, and left to UV light for 30 minutes under nitrogen. After curing completed, PTMC film was peeled away from the PFPE mold. Second method was particle harvesting by means of an adhesive layer. Particles in the mold was covered with an adhesive layer which is cyanoacrylate based super glue on a flexible PDMS backing. After the glue was dried, PDMS was peeled away from the mold and adhesive layer was solved in acetone. Lastly, a simpler method was applied which is sonication. The mold with the cured particles was put in DCM and left on sonication bath for a one day. After filtration of the solution by Chromafil® syringe filters, PTMC based particles were harvested on the filter paper.

3.4. Characterization Methods

Number average molecular weight ($\bar{M}_n$), weight average molecular weight ($\bar{M}_w$) and polydispersity index (PDI) of high molecular weight PTMC were determined by means of Polymer Laboratories PL-GPC 220 gel permeation chromatography (GPC) instrument using chloroform as eluent with the flow rate of 1.0 mL/min at room temperature. Determination of repeating unit, conversion of TMC monomer, functionalization of two- or three-armed PTMC oligomers and molecular weights of these oligomers were carried out with Bruker AVANCE III 400 MHz proton nuclear magnetic resonance (^{1}H-NMR) spectroscopy by dissolving in deuterated chloroform ($CDCl_3$). Particle morphology was imaged by QUANTA 400F Field Emission SEM instrument by coating with 5 nm gold-palladium alloy.

CHAPTER 4

RESULTS AND DISCUSSIONS

4.1. Poly(trimethylene carbonate) Oligomer Synthesis

The synthesis of methacrylate functionalized PTMC oligomers was shown in Figure 4.1.1. TMC was polymerized in the presence of trimethylol propane initiator to obtain three-armed PTMC oligomers. The repeating unit of the oligomers was planned to be three for each arm, calculated from the molar ratio of TMC to trimethylol propane.

After synthesis, the molecular weight of the oligomers was calculated from the ^{1}H-NMR spectra, assuming that each hydroxyl group of the trimethylol propane starts polymerization of TMC. An example of the spectrum was shown in Figure 4.1.2. The integral of peak near 0.90 ppm belongs to $–CH_3$ group at initiator (indicated as (a) in Figure 4.1.2), whereas the integral of peak close to 4.20 ppm belongs to $–CH_2$ group at the repeating unit (indicated as (b) in Figure 4.1.2). Triplet close to 2.10 ppm also represents $–CH_2$ group at the repeating unit (indicated as (c) in Figure 4.1.2). According to the ratio between repeating unit and initiator, repeating units of three-armed PTMC oligomers were calculated between 2.5-2.7. After synthesizing hydroxyl-terminated PTMC oligomers, they were functionalized with excess methacryloyl chloride to obtain crosslinking agent (Figure 4.1.1b). The methacrylate groups were observed around 6.10 ppm (-CH-), 5.50 ppm (-CH-) ((d) in Figure 4.1.3) and close to 2.00 ppm ($-CH_3$) ((e) in Figure 4.1.3). Degree of functionalization was calculated above 85% by

comparing the area of the methacrylate peak at 6.10 ppm and PTMC oligomer peak at 4.20 ppm ((b) in Figure 4.1.2.).

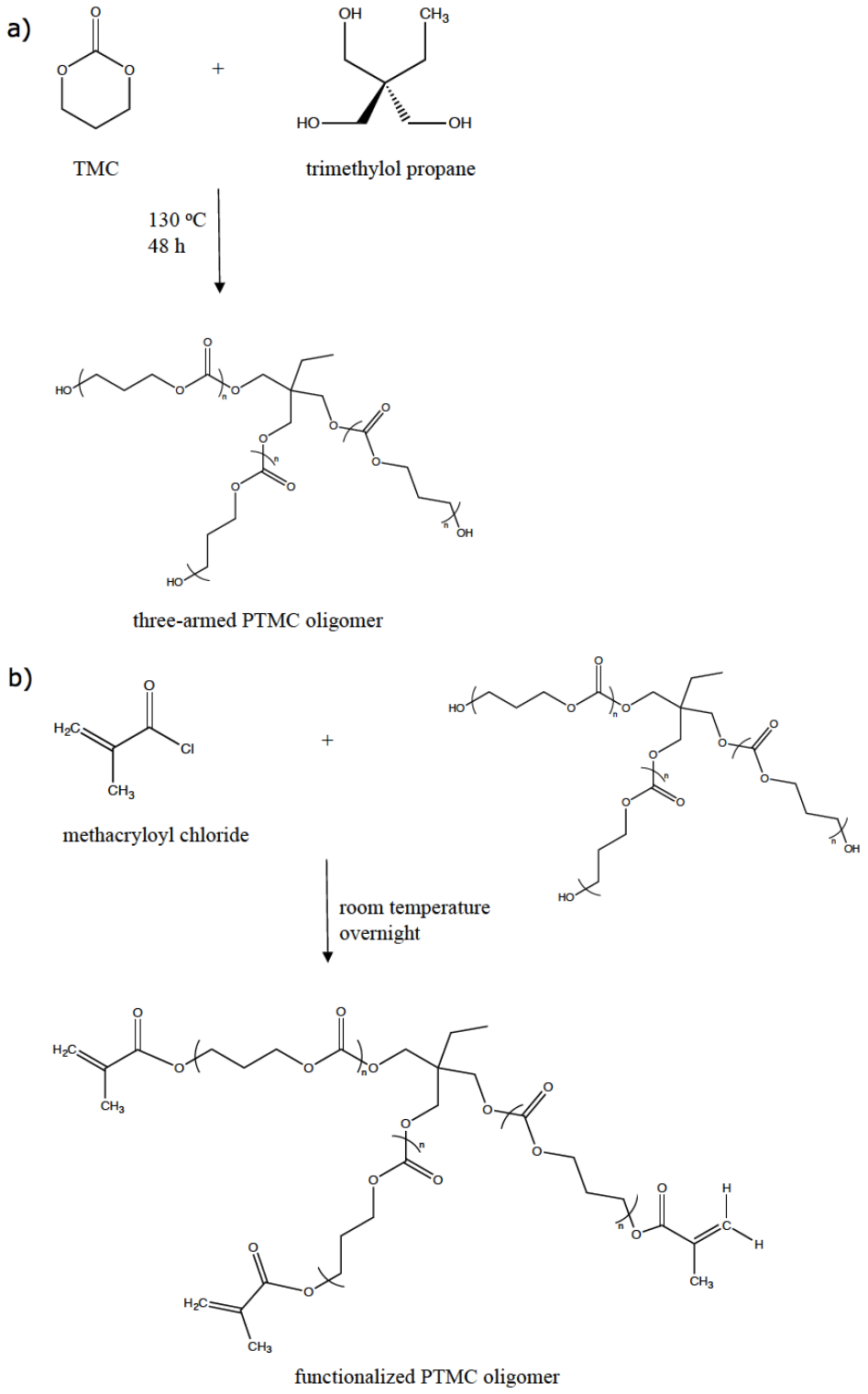

Figure 4.1.1 Schematic diagram showing a) synthesis of three-armed hydroxyl

terminated PTMC oligomers by using trimethylol propane initiator, b) functionalization of three-armed PTMC oligomers with methacryloyl chloride

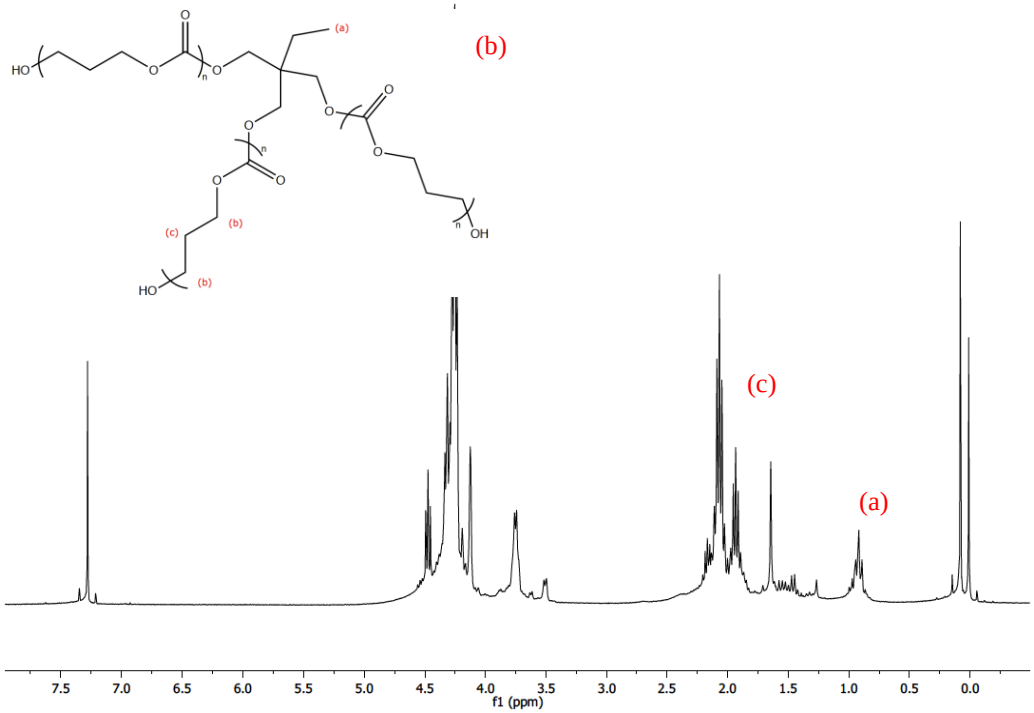

Figure 4.1.2 Characteristic ^{1}H NMR spectrum of three-armed PTMC oligomers

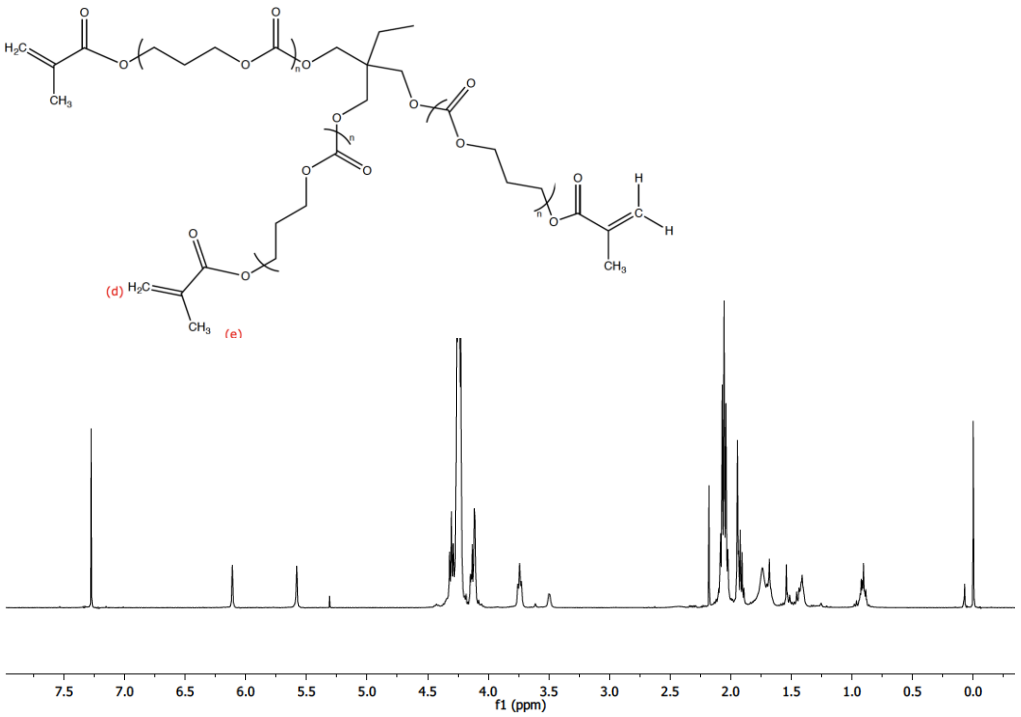

Figure 4.1.3 Characteristic ^{1}H NMR spectrum of functionalized three-armed PTMC oligomers

4.2. Elastomeric Network Preparation

High molecular weight PTMC was synthesized by ring opening polymerization of the TMC monomer in the presence of stannous octoate catalyst at 130 °C for three days under nitrogen (Figure 4.2.1). $\overline{M}_n$ and $\overline{M}_w$ values are found as 183,656 and 343,363 g/mol, respectively and PDI was calculated as 1.87.

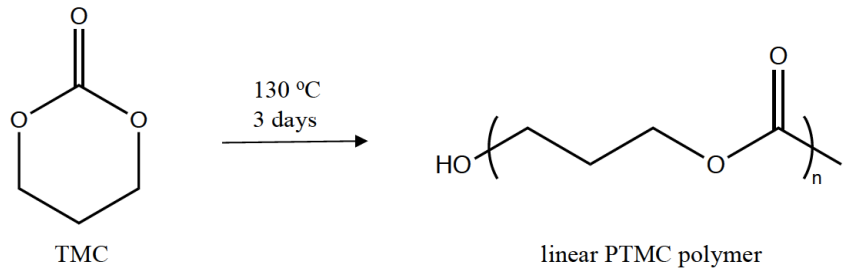

Figure 4.2.1 Linear high molecular weight PTMC synthesis by ring opening polymerization of TMC monomer

High molecular weight PTMC was homogenously mixed with PTMC oligomer and photoinitiator to obtain PTMC based film.

4.3. Perfluoropolyether Micropatterned Mold Fabrication

To obtain particles with precise shape and size without formation of scum layer, photocurable PFPE based elastomeric mold fabrication was done. PFPE is a viscous fluoropolymer with $-(CF_2CF_2O)_m-(CF_2O)_n-$ repeating unit [49]. It has low surface energy, low toxicity, high durability and extremely resistant to organic solvents [49], [104], [105]. Thanks to its high spreading coefficient, PFPE can totally cover the surface of patterned wafer (Figure 4.3.1a) and after photocuring, replica PFPE mold was obtained (Figure 4.3.1b-c). One of the most attractive feature of fluoro-based polymers in soft-lithography applications are pattern fidelity and high resolution without any deformation on the patterns [105]. Under favor of these properties, inverse pattern without any damage can be observed on the replica mold as shown in Figure 4.3.1b.

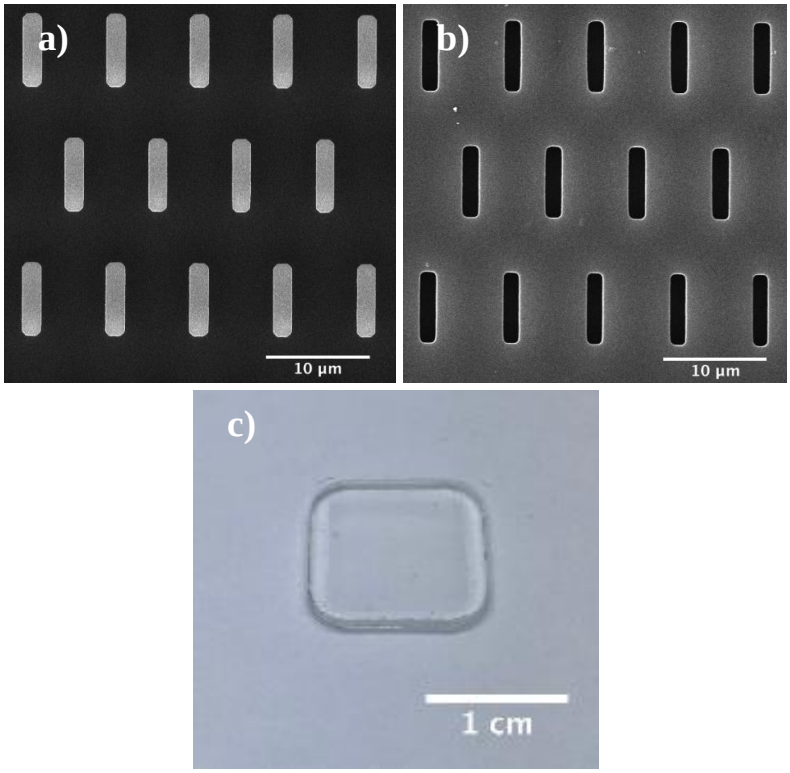

Figure 4.3.1 a) SEM images of 2 x 8 μm^2 rectangle protrusions produced on silicon wafer by lithographic techniques, b) SEM images of replicated PFPE mold (2 x 8 μm^2 rectangle indentation with 2 µm depth), and c) digital photography of a PFPE mold with patterned surface.

It is possible to obtain molds containing indentations in different patterns and sizes depending on the mask obtained by lithographic methods. In this study, in addition to rectangle, circles and square patterns with diameters ranging from 2 to 100 µm were fabricated (Figure 4.3.2).

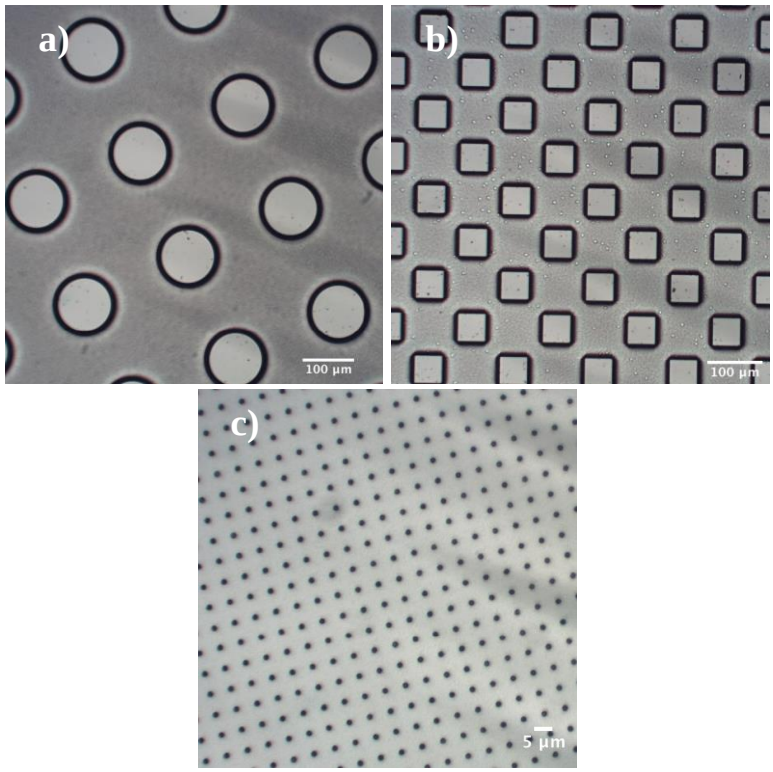

Figure 4.3.2 Optical microscope images of PFPE molds with dimensions of a) 100 μm circle, b) 50 μm square, c) 2 μm circle

4.4. Poly(trimethylene carbonate) Based Microparticle Fabrication

In a typical PRINT process to obtain free particles, roll to roll system was used [9], [106]. In this system, once the pre-particle material is filled into the wells, a roller passes by applying pressure on the non-wetting mold and wipe the excess material out on the surface of the mold to prevent scum layer formation. Here, however, without using such a system, various methods have been tried to obtain isolated particles.

Primarily, high molecular weight PTMC based isolated particles were tried to fabricate via NIL device. The prepared PTMC film was placed between flat PFPE surface and mold. By increasing temperature and applying higher pressure, molten polymer filled into patterns. However, even when the amount of polymer was insufficient to fill all the indentations, free-standing particles

could not be obtained with this method and as seen from Figure 4.4.1, patterned film was fabricated. The reason may be due to contact problem between mold and flat surfaces. It may be useful to produce finer molds so that the surfaces will sit more tightly together. As an alternative approach, closer pattern gaps may be preferred as they can assist in splitting the film layer.

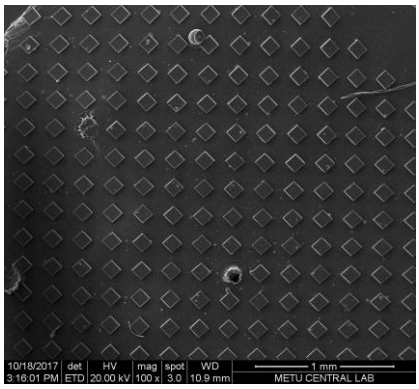

Figure 4.4.1 SEM image of NIL printed 100 μm cubic pillars on PTMC film

Once it was realized that free particles could not be produced using PTMC film, instead, viscous PTMC resin was used. After placing flat-PDMS/PTMC/patterned-PDMS sandwich structure in NIL device and curing, PTMC drops were observed onto flat PDMS surface (Figure 4.4.2).

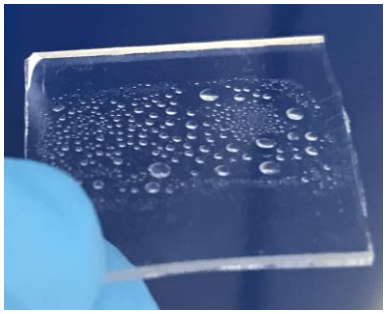

Figure 4.4.2 PTMC drops formation onto flat PDMS surface after curing in NIL device

In Figure 4.4.2, the appearance of droplets instead of free-standing PTMC particles on a flat surface indicates that the sandwich structure placed on the NIL device was not uniformly pressurized by the device. Therefore, the mold cavities were not properly filled and the oligomer could not get the desired particle shape.

Same procedure was repeated with flat-PFPE/PTMC/patterned-PFPE with glass slide backing. Although the glass was coated with chemical vapor decomposition of methacrylate, the reverse patterned PFPE film was stripped from the glass surface and could not be used, as it would be cleaned with an organic solvent such as ethanol. So, flat-PFPE/PTMC/patterned-PFPE sandwich structure was tested in NIL device to obtain isolated PTMC particles. Although oligomers could easily flow through cavities due to their viscosities and by the help of pressure applied, still film layer formation was observed after crosslinking (Figure 4.4.3). The reason may be again due to the fact that the mold and the surface placed on the NIL device were not in good contact. Even high pressure was applied, the resin was not distributed uniformly and excess material could not move on the mold edges.

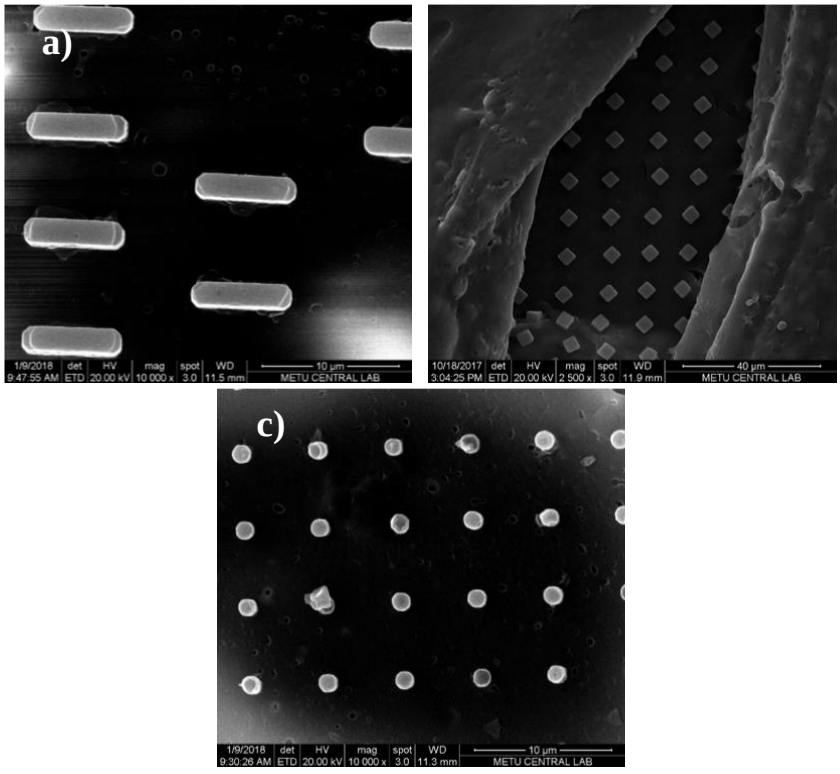

Figure 4.4.3 SEM images of PTMC based micro particles on the film layer fabricated using NIL. a) 2 x 8 μm^2 rectangle, b) 5 µm cube and c) 2 µm cylinder.

According to the experiments conducted using imprint device, it was understood that excess material on patterned mold surface should be swept after filling mold cavities to prevent formation of film layer.

The patterned surface of the PFPE mold was swept with a flat PFPE surface once filling the mold with pre-particle material. Here, instead of obtaining isolated particles, even a uniform shape could not be observed. Moving smooth fluoro-based surface on the mold interconnected the material inside the cavities by forming a layer on it as presented in Figure 4.4.4.

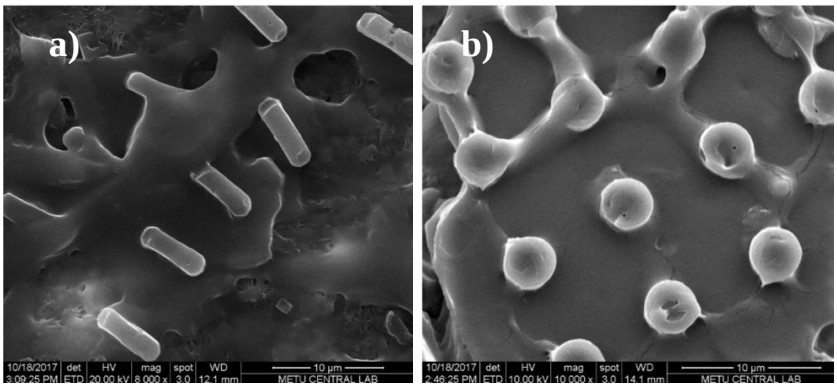

Figure 4.4.4 SEM images of a) 2 x 8 μm^2 rectangle, b) 5 μm cylinder particles with scum layer

Alternatively, the treatment was repeated using a sharp blade. After the material was covered the surface of patterned mold, flat side of a sharp edge blade was gently moved along it. Among the other methods, the formation of residue was totally prevented. Nevertheless, since it was a manual application and the depth of the blade movement could not be controlled, some of the pre-particle resin was taken inside the indentations and after photocrosslinking, holes were observed in the particles as shown in Figure 4.4.5.

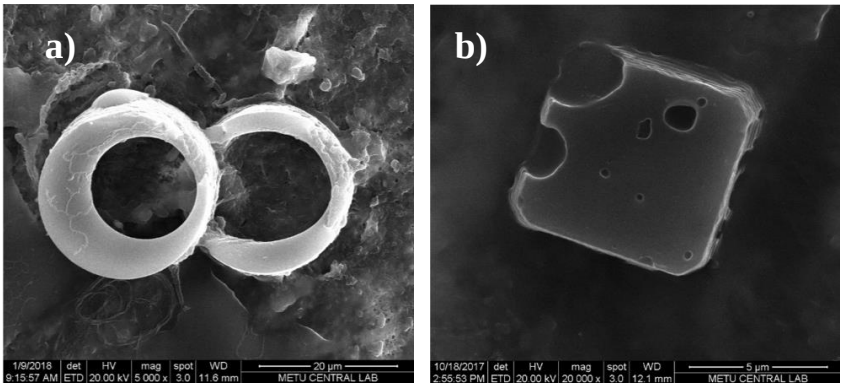

Figure 4.4.5 Perforated free PTMC particles with precise shape and size. a) 25 µm cylinder, c) 8 µm cube

Since successful results cannot be achieved from different sweeping methods, a completely different path was followed. The patterned mold was coated with dilute resin by spinning. Here, it was aimed that the cavities would be completely filled with PTMC resin and since the surface outside the cavities have a non-wetting nature, the residue would not be observed. As expected, all the cavities were filled properly. Figure 4.4.6 demonstrates the most successful examples of this method. Although not much observed in particles of 100 µm and 50 µm in size, some of the particles with diameters of 25 µm and below were found to have residual material due to spinning. In Figure 4.4.6a, lateral dimension of the bottom part of cylinder was approximately 25 µm, whereas top of it was approximately 44 µm. Hence, the particle appeared like mushroom instead of cylindrical. In Figure 4.4.6b, as another example, free 25 µm cubic particle was obtained with a layer on the bottom. With smaller patterns, possibility of residual layer formation increased. Consequently, free particles were noticed with scum layer (Figure 4.4.6c). Besides, 2 µm particle diameters could not be obtained using spin coater because of film formation.

Among all the methods applied, Mayer rod gave the best results by spreading the resin evenly. Whilst rolling the rod, the cavities were filled since each turn of wire was directly in contact with contiguous turn. The contact between them formed the groove, which was involved in filling the cavities. Thus, PTMC based micro particles in various shape and diameter were produced (Figure 4.4.7).

To obtain free-standing particles, they had to be separated from the mold and collected in solvent as an eventual step of particle fabrication. Therefore, PTMC film was placed in contact with PTMC oligomers filling the pattern of the mold, and left to UV light. Cured particles prefer to stick to the PTMC film instead of staying on the PFPE surface. However, separation of cured particles from PTMC film was the main problem. As an alternative method, the mold was covered with a cyanoacrylate based adhesive layer. After the adhesive layer was peeled away from the mold, it was solved in acetone. Since crosslinked PTMC particles was not soluble into acetone, free standing particles were collected. Nevertheless, this method was abandoned due to the possibility that polymer particles may still have cyanoacrylate residues which can cause the formation of toxic formaldehyde by degradation [107]. Thus, a simpler method was applied which is sonication. The mold with the cured particles was put in DCM and left on sonication bath for a whole day. After filtration of the solution, PTMC based particles were harvested on filter paper. Even if the separation of PTMC based particles using sonication was the easiest method, it was highly time-consuming process. Moreover, it was not effective enough to remove all the particles from the mold cavities (Figure 4.4.8). Hence, after filtration, limited number of particles were dispersed on the surface of the filter paper and a group of free particle formation was not easily detected in the SEM images. Another drawback of this method was using filter paper again due to the limited number of particles. After evaporation of solvent, dried particles fell from smooth surfaces like aluminum foil. However, the filter paper did not allow the particles to be poured out because the dry particles could easily hold on the filter paper. On account of the filter paper, there was no clear background in SEM images.

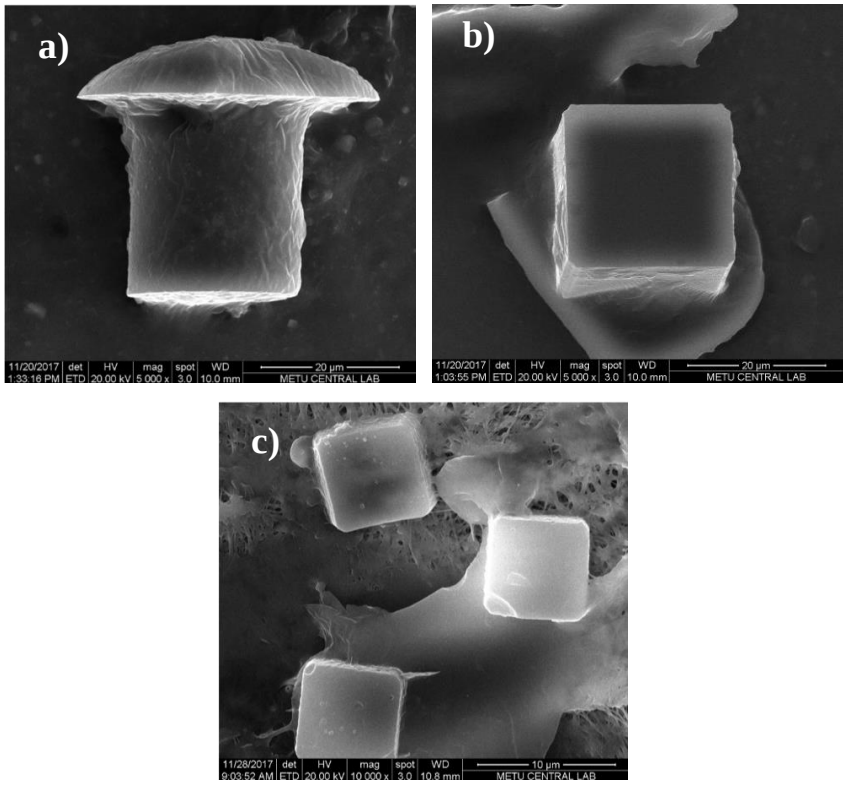

Figure 4.4.6 SEM images o PTMC particles with scum layer fabricated by spin coating. a) 25 µm cylindrical particle seem like mushroom, b) 25 µm cube with residual layer, c) 8 µm cubic free particle and particles with scum layer

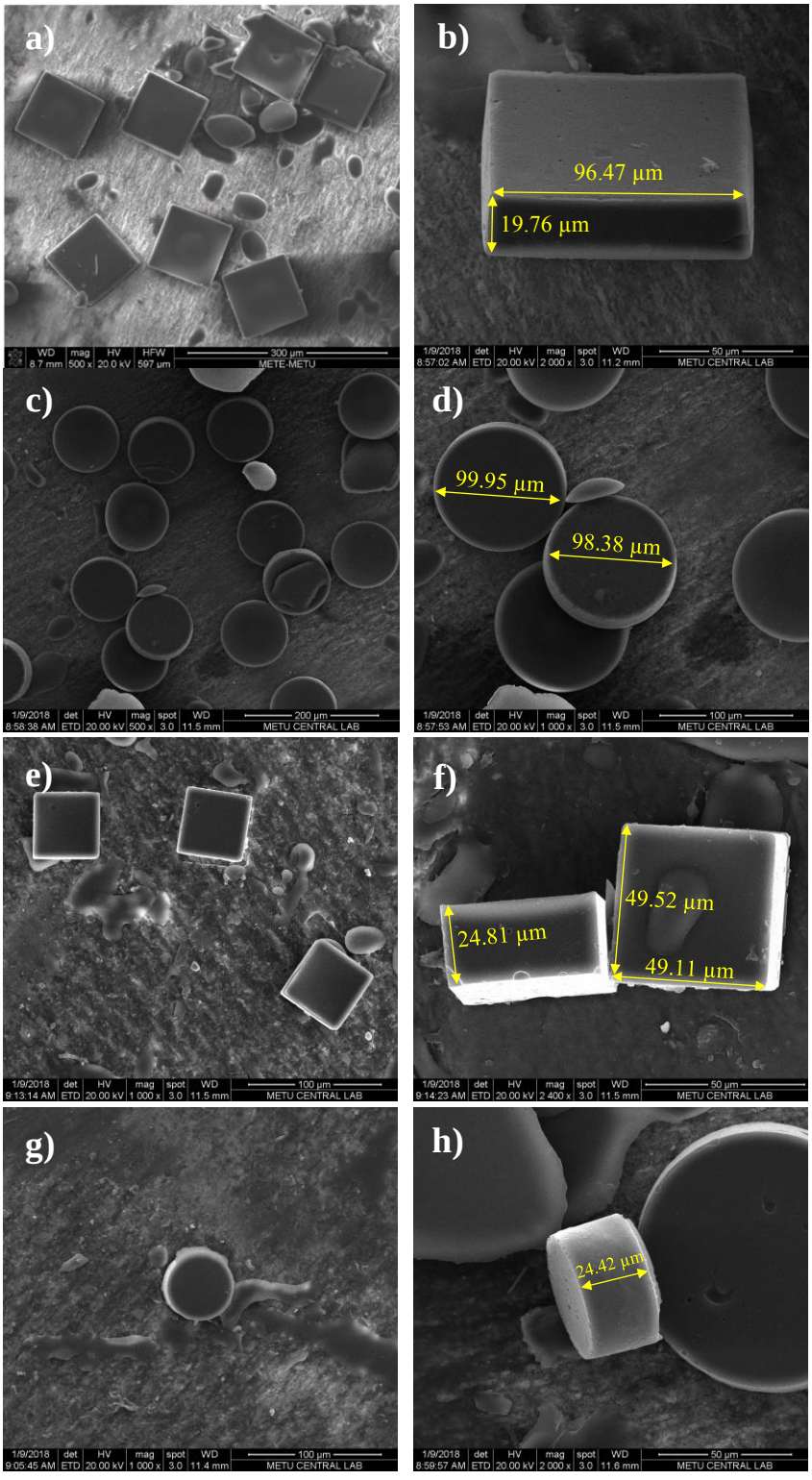
a)
b)
96.47 µm
19.76 µm
c)
d)
99.95 µm
98.38 µm
e)
f)
49.52 µm
24.81 µm
49.11 µm
g)
h)
24.42 µm

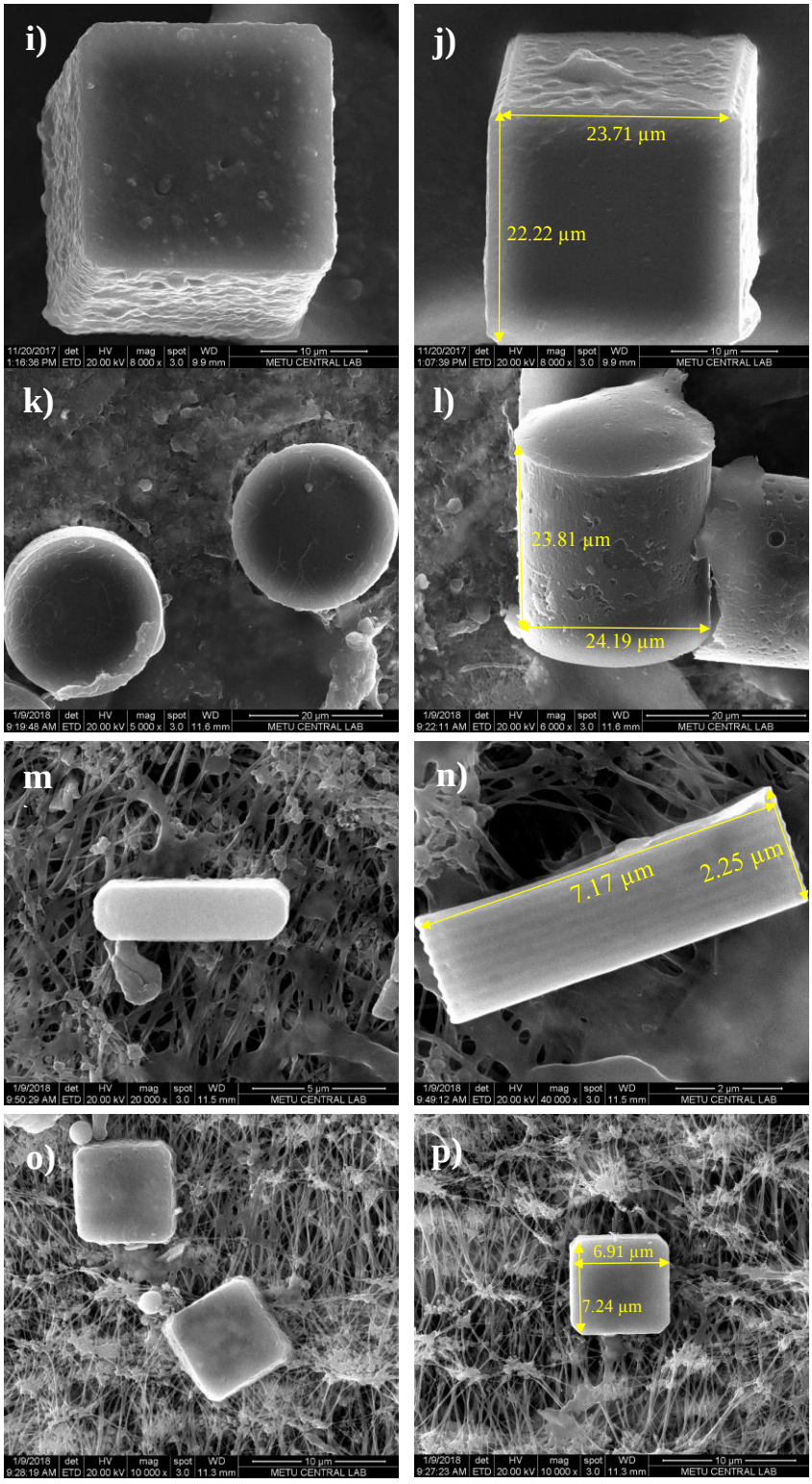
i)
j)
23.71 µm
22.22 µm
k)
l)
23.81 µm
24.19 µm
m
n)
7.17 µm
2.25 µm
o)
p)
6.91 µm
7.24 µm

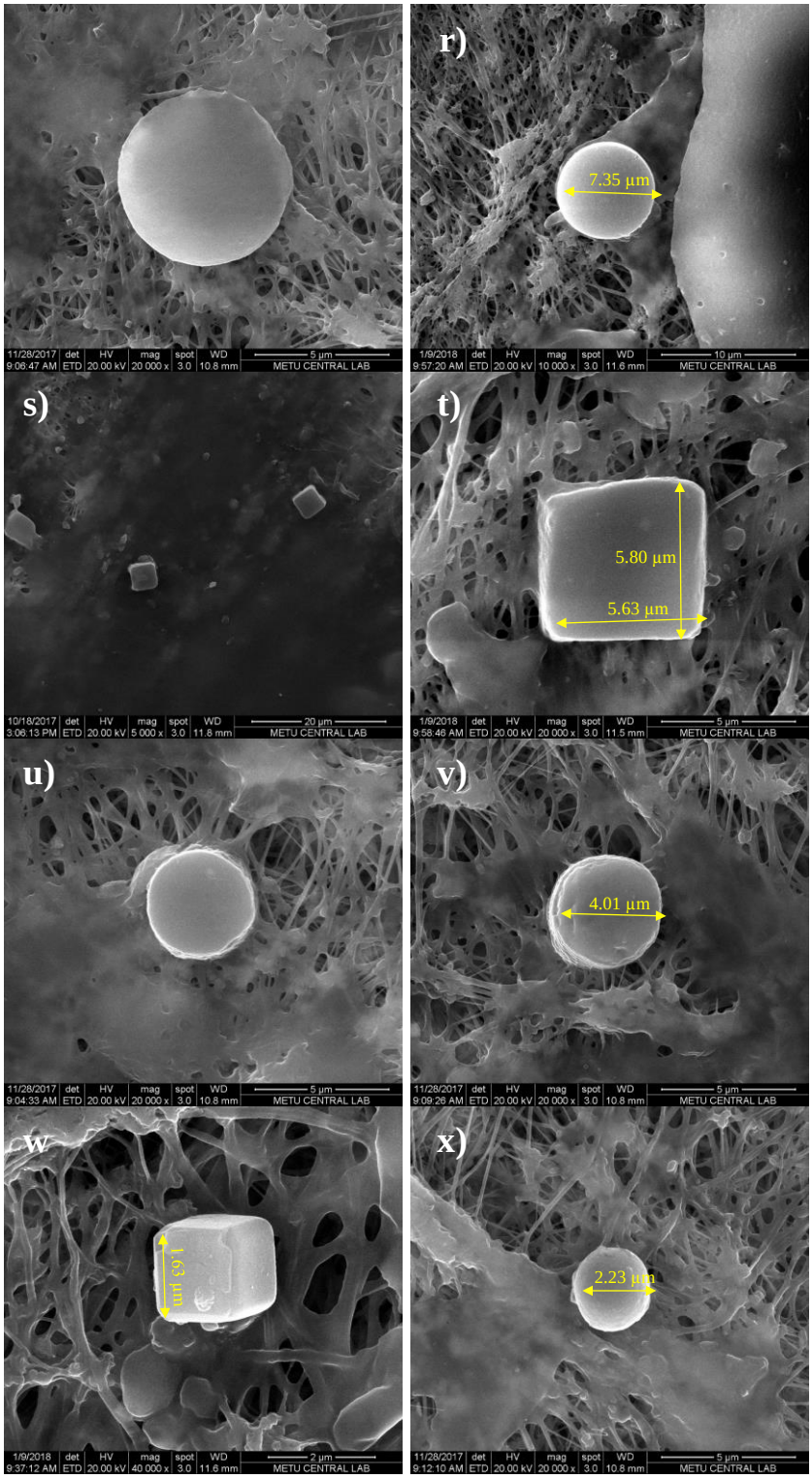

Figure 4.4.7 SEM images of isolated PTMC particles harvested on filter paper after fabricated by Mayer rod coater. (a-b) 100 µm cube, (c-d) 100 µm cylinder, (e-f) 50 µm cube, (g-h) 50 µm cylinder, (i-j) 25 µm cube, (k-l) 25 µm cylinder,

(m-n) 8 x 2 μm^2 rectangle, (o-p) 8 µm cube, (q-r) 8 µm cylinder, (s-t) 5 µm cube, (u-v) 5 µm cylinder, w) 2 µm cube and x) 2 µm cylinder.

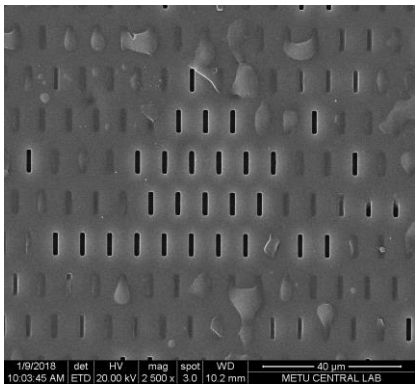

Figure 4.4.8 SEM image of used rectangle PFPE mold. After sonication, a major part of the mold cavities was still full with PTMC particles.

After improving especially the harvesting method drawbacks, biocompatible PTMC based particles can be used in drug delivery applications as micro carriers. Moreover, PTMC based micro carriers with various size and shape can be fabricated by preparing silicon mask contains different size and patterns by lithographic techniques.

CHAPTER 5

CONCLUSIONS

PTMC based microparticle fabrication by using PRINT technique have been demonstrated. Using lithographic methods, silicon wafer with protrusions in certain sizes and shapes were obtained. Non-wetting replica of this mask with indented patterns was produced. Meanwhile, three-armed viscous PTMC oligomers were synthesized and end groups were functionalized to achive a networked structure after photocuring. Several techniques have been tried to fill the cavities with viscous oligomers without formation any scum layer. Even if the viscous material under certain pressure was allowed to fill all the cavities using NIL device, a film layer on the surface was observed. Flat PFPE surface was swept through the surface of the mold to clean excess material but still completely isolated particles could not be obtained and scum layer was observed. Besides, the flat side of a sharp blade was gently moved over the mold surface, yet holes were observed in the middle of the particles. Among them, the best results were obtained from spin coater and #1 Mayer rod. Isolated particles with 100, 50 and 25 μm diameter were procured both using spin coater and Mayer rod but particles with smaller diameter such as 8, 5 and 2 μm were fabricated much more precisely using Mayer rod. Harvesting method of particles was another key point to gather whole isolated particles. Overlaid PFPE mold with PTMC based film and crosslinked together, all free-standing particles was preferred to stick film instead of mold but particles were not successfully separated from the surface of the film. An adhesive layer was used and again particles were totally collected. However, it was in doubt that adhesive layer was totally removed from the particle surface. So, a simpler method was preferred

and isolated particles were took out from the mold by sonication. Eventually, PTMC based particles in cube and cylinder shape with ranging diameters between 2 – 100 μm and 2 x 8 μm rectangle were fabricated by using PRINT technique to use in controlled drug delivery applications.

CHAPTER 6

RECOMMENDATIONS

According to the studies conducted, a few suggestions are presented for the future work. Instead of using thick PFPE mold, fluorocur can be spread over a backing sheet which should have high surface energy to enable smooth adhesion. Thereby, contact problems using NIL may be overcome. Sub-micron sized, sharp edge patterns such as asterisk, diamond, triangle can be designed and PTMC oligomers with different shape and size can be produced using NIL. Another recommendation is about harvesting method. Instead of the sonication, it can be collected with the aid of an adhesive layer that does not create any toxic effects or purification from adhesive layer residue may be improved. Thus, the number of free particles will be increased and fabricated PTMC based particles may become appropriate for controlled drug release applications.

REFERENCES

[1] Y. Zhang, H. F. Chan and K. W. Leong, "Advanced Materials and Processing for Drug Delivery: The Past and the Future," *Advanced Drug Delivery Reviews*, vol. 65, no. 1, pp. 104-120, 2013.

[2] C. G. Wilson, "The Need for Drugs and Drug Delivery Systems," in *Fundamentals and Applications of Controlled Release Drug Delivery*, London, Springer, 2012, pp. 3-18.

[3] G. Tiwari, R. Tiwari, B. Sriwastawa, L. Bhati, S. Pandey, P. Pandey and S. K. Bannerjee, "Drug delivery systems: An updated review," *International Journal of Pharmaceutical Investigation*, vol. 2, no. 1, pp. 2-11, 2012.

[4] A. T. Florence, "A Short History of Controlled Drug Release and an Introduction," in *Controlled Release in Oral Drug Delivery*, London, Springer, 2011, pp. 1-20.

[5] M. Grissinger, "The Five Rights A Destination Without a Map," *Pharmacy and Therapeutics*, vol. 35, no. 10, p. 542, 2010.

[6] M. W. Tibbitt, J. E. Dahlman and R. Langer, "Emerging Frontiers in Drug Delivery," *Journal of the American Chemical Society*, vol. 138, pp. 704-714, 2016.

[7] I. Negut, V. Grumezescu, G. Dorcioman and G. Socol, "Microscale Drug Delivery Systems: Current Perspectives and Novel Approaches," in *Nano- and Microscale Drug Delivery Systems Design and Fabrication*, Elsevier, 2017, p. 2.

[8] Z. Abdullaeva, Synthesis of Nanoparticles and Nanomaterials: Biological Approaches, Springer, 2017, pp. 3-4.

[9] J. Xu, D. H. C. Wong, J. D. Byrne, K. Chen, C. Bowerman and J. M. DeSimone, "Future of the Particle Replication in Nonwetting Templates (PRINT) Technology," *Angewandte Chemie International Edition,* vol. 57, p. 6580 – 6589, 2013.

[10] J. A. Champion, Y. K. Katare and S. Mitragotri, "Particle shape: A new design parameter for micro- and nanoscale drug delivery carriers," *Journal of Controlled Release,* vol. 121, no. 1-2, pp. 3-9, 2007.

[11] J. P. Rolland, B. W. Maynor, L. E. Euliss, A. E. Exner, G. M. Denison and J. M. DeSimone, "Direct Fabrication and Harvesting of Monodisperse, Shape-Specific Nanobiomaterials," *Journal of the American Chemical Society,* vol. 127, no. 28, p. 10096–10100, 2005.

[12] B. D. Ulery, L. S. Nair and C. T. Laurencin, "Biomedical Applications of Biodegradable Polymers," *Journal of Polymer Science Part B: Polymer Physics,* vol. 49, no. 12, pp. 832-864, 2011.

[13] B. A. Aderibigbe and H. E. Mukaya, "Polymer Therapeutics Design, Application, and Pharmacokinetics," in *Nano- and Microscale Drug Delivery Systems: Design and Fabrication,* Elsevier, 2017, pp. 33-44.

[14] K. Fukushima, "Poly(trimethylene carbonate)-based polymers engineered for biodegradable functional biomaterials," *Biomaterials Science,* vol. 4, no. 9, pp. 9-24, 2016.

[15] K. E. Uhrich, S. M. Cannizzaro and R. S. Langer, "Polymeric Systems for Controlled Drug Release," *Chemical Reviews,* vol. 99, no. 11, pp. 3181-3198, 1999.

[16] R. Langer, "Drug delivery and targeting," *Nature,* vol. 392, no. 6679, pp. 5-10, 1998.

[17] R. A. Siegel and M. J. Rathbone, "Overview of Controlled Release Mechanisms," in *Fundamentals and Applications of Controlled Release Drug Delivery,* Springer, 2012, pp. 20-21.

[18] D. Bhowmik, H. Gopinath, P. B. Kumar, S. Duraivel and S. K. P. Kumar, "Controlled Release Drug Delivery Systems," *The Pharma Innovation,* vol. 1, no. 10, p. 24, 2012.

[19] J. Siepmann and F. Siepmann, "Microparticles Used as Drug Delivery Systems," *Progress in Colloid and Polymer Science,* vol. 133, pp. 15-21, 2006.

[20] C. Evora, I. Soriano, R. A. Rogers, K. M. Shakesheff, J. Hanes and R. Langer, " Relating the phagocytosis of microparticles by alveolar macrophages to surface chemistry: the effect of 1,2-dipalmitoylphosphatidylcholine," *Journal of Controlled Release,* vol. 51, pp. 143-152, 1998.

[21] C. R. Dass and M. A. Burton, "Microsphere-mediated targeted gene therapy of solid tumors," *Drug Delivery,* vol. 6, pp. 243-252, 1999.

[22] L. Brannon-Peppas, "Recent advances on the use of biodegradable microparticles and nanoparticles in controlled drug delivery," *Interntional Journal of Pharmaceutics,* vol. 116, pp. 1-9, 1995.

[23] Y. Xia and D. W. Pack, " Uniform biodegradable microparticle systems for controlled release," *Journal of Controlled Release,* vol. 18, no. 82, pp. 137-147, 2002.

[24] N. Nishiyama, "Nanocarriers shape up for long life," *Nanomedicine,* vol. 2, p. 203, 2007.

[25] S. E. Gratton, P. A. Ropp, P. D. Pohlhaus, C. J. Luft, V. J. Madden, M. E. Napier and J. M. DeSimone, "The effect of particle design on cellular

internalization pathways," *Proceedings of the National Academy of Science,* vol. 105, no. 33, pp. 11613-11618, 2008.

[26] P. Decuzzi, F. Causa, M. Ferrari and P. A. Netti, "The Effective Dispersion of Nanovectors Within the Tumor Microvasculature," *Annals of Biomedical Engineering,* vol. 34, no. 4, pp. 633-641, 2006.

[27] G. L. Hornyak, J. Dutta, H. F. Tibbals and A. K. Rao, "Fabrication Methods," in *Introduction to Nanoscience*, CRC Press, 2008, pp. 178-224.

[28] M. Caldorera-Moore, N. Guimard, L. Shi and K. Roy, "Designer nanoparticles: Incorporating size, shape, and triggered release into nanoscale drug carriers," *Expert Opinion on Drug Delivery,* vol. 7, no. 4, pp. 479-495, 2010.

[29] C. K. Preston and M. Moskovits, "Optical Characterization of Anodic Aluminum Oxide Films Containing Electrochemically Deposited Metal Particles," *The Journal of Physical Chemistry,* vol. 97, no. 32, pp. 8495-8503, 1993.

[30] X. Chen, S. Yeganeh, L. Qin, S. Li, S. Xue, C. Xue, A. B. Braunschweig, G. C. Schatz, M. A. Ratner and C. A. Mirkin, "Chemical Fabrication of Heterometallic Nanogaps for Molecular Transport Junctions," *Nano Letters,* vol. 9, no. 12, pp. 3974-3979, 2009.

[31] S. J. Hurst, E. Kathryn Payne, L. Qin and C. A. Mirkin, "Multisegmented One-Dimensional Nanorods Prepared by Hard-Template Synthetic Methods," *Angewandte Chemie International Edition,* vol. 45, no. 17, pp. 2672-2692, 2006.

[32] J.-W. Yoo and S. Mitragotri, "Polymer particles that switch shape in response to a stimulus," *Proceedings of the National Academy of Sciences,* vol. 107, no. 25, p. 11205–11210, 2010.

[33] C. C. Ho, A. Keller, J. A. Odell and R. H. Ottewill, "Preparation of monodisperse ellipsoidal polystyrene particles," *Colloid and Polymer Science*, vol. 271, pp. 469-479, 1993.

[34] J. A. Champion, Y. K. Katare and S. Mitragotri, "Making polymeric micro- and nanoparticles of complex shapes," *Proceedings of the National Academy of Sciences of the United States of America,* vol. 104, no. 29, p. 11901–11904, 2007.

[35] Z. Nie, S. Xu, M. Seo, P. C. Lewis and E. Kumacheva, " Polymer Particles with Various Shapes and Morphologies Produced in Continuous Microfluidic Reactors," *Journal of the American Chemical Society,* vol. 127, no. 22, pp. 8058-8063, 2005.

[36] D. Dendukuri, S. S. Gu, D. C. Pregibon, A. Hatton and P. S. Doyle, "Stop-flow lithography in a microfluidic device," *Lab on a Chip,* vol. 7, no. 7, pp. 818-828, 2007.

[37] C. Decker and A. D. Jenkins, "Kinetic approach of oxygen inhibition in ultraviolet- and laser-induced polymerizations," *Macromolecules,* vol. 18, no. 6, pp. 1241-1244, 1985.

[38] P. Panda, K. P. Yuet, T. A. Hatton and P. S. Doyle, "Tuning Curvature in Flow Lithography: A New Class of Concave/Convex Particles," *Langmuir,* vol. 25, no. 10, pp. 5986-92, 2009.

[39] S.-H. Kim, J. W. Shim, J.-M. Lim, S. Y. Lee and S.-M. Yang, "Microfluidic fabrication of microparticles with structural complexity

using photocurable emulsion droplets," *New Journal of Physics*, vol. 11, pp. 2-16, 2009.

[40] G. F. Christopher and S. L. Anna, "Microfluidic methods for generating continuous droplet streams," *Journal of Physics D: Applied Physics*, vol. 40, p. R319–R336, 2007.

[41] M. Geissler and Y. Xia, "Patterning: Principles and Some NewDevelopments," *Advanced Materials*, vol. 16, no. 15, pp. 1249-1269, 2004.

[42] S. V. Sreenivasan, "Nanoscale Manufacturing Enabled by Imprint Lithography," *Special Issue: Nanostructured Materials in Information Storage MRS Bulletin*, vol. 33, pp. 854-863, 2008.

[43] S. Badaire, C. Cottin-Bizonne and A. D. Stroock, "Experimental Investigation of Selective Colloidal Interactions Controlled by Shape, Surface Roughness, and Steric Layers," *Langmuir*, vol. 24, no. 20, pp. 11451-11463, 2008.

[44] C. J. Hernandez and T. G. Mason, "Colloidal Alphabet Soup: Monodisperse Dispersions of Shape-Designed LithoParticles," *The Journal of Physical Chemistry C*, vol. 111, no. 12, pp. 4477-4480, 2007.

[45] C. J. Hernandez, K. Zhao and T. G. Mason, "Well-Deposition Particle Templating: Rapid Mass-Production of LithoParticles Without Mechanical Imprinting," *Soft Materials*, vol. 5, no. 1, pp. 13-31, 2007.

[46] Y. Xia and G. M. Whitesides, "Soft Lithography," *Angewandte Chemie*, vol. 37, no. 5, p. 550–575, 1998.

[47] J. Dumond and H. Y. Low, "Residual Layer Self-Removal in Imprint Lithography," *Advanced Materials*, vol. 20, no. 7, p. 1291–1297, 2008.

[48] L. C. Glangchai, M. Caldorera-Moore, L. Shi and K. Roy, "Nanoimprint lithography based fabrication of shape-specific, enzymatically-triggered smart nanoparticles," *Journal of Controlled Release,* vol. 125, no. 3, pp. 263-272, 2008.

[49] J. P. Rolland, R. M. Van Dam, D. A. Schorzman , S. R. Quake and J. M. DeSimone, "Solvent-Resistant Photocurable “Liquid Teflon” for Microfluidic Device Fabrication," *Journal of American Chemical Society,* vol. 126, no. 8, p. 2322–2323, 2004.

[50] M. W. Benjamin, L. Isaac , H. Zhaokang, J. P. Rolland, A. Pandya, Q. Fu, J. Liu, R. J. Spontak, S. S. Sheiko, R. J. Samulski, E. T. Samulski and J. M. DeSimone, "Supramolecular Nanomimetics: Replication of Micelles, Viruses, and Other Naturally Occurring Nanoscale Objects," *Small,* vol. 3, no. 5, p. 845 – 849, 2007.

[51] Y. Xia, J. A. Rogers, K. E. Paul and G. M. Whitesides, "Unconventional Methods for Fabricating and Patterning Nanostructures," *Chemical Reviews,* vol. 99, no. 7, p. 1823−1848, 1999.

[52] T. J. Merkel, K. P. Herlihy, J. Nunes, R. M. Orgel, J. P. Rolland and J. M. DeSimone, "Scalable, Shape-specific, Top-down Fabrication Methods for the Synthesis of Engineered Colloidal Particles," *Langmuir,* vol. 26, no. 16, p. 13086–13096, 2010.

[53] B. D. Gates, Q. Xu, M. Stewart, D. Ryan, C. G. Willson and G. M. Whitesides, "New Approaches to Nanofabrication: Molding, Printing, and Other Techniques," *Chemical Reviews,* vol. 105, no. 4, p. 1171–1196, 2005.

[54] "Photolithography," Cellular and molecular biomechanics laboratory, [Online]. Available: http://biomechanicalregulation-lab.org/photolithography/. [Accessed 19 July 2017].

[55] S. E. A. Gratton, S. S. Williams, M. E. Napier, P. D. Pohlhaus, Z. Zhou, K. B. Wiles, B. W. Maynor, C. Shen, T. Olafsen, E. T. Samulski and J. M. DeSimone, "The Pursuit of a Scalable Nanofabrication Platform for Use in Material and Life Science Applications," *Accounts of Chemical Research,* vol. 41, no. 12, pp. 1685-1695, 2008.

[56] K. P. Herlihy, J. Nunes and J. M. DeSimone, "Electrically Driven Alignment and Crystallization of Unique Anisotropic Polymer Particles," *Langmuir,* vol. 24, no. 16, pp. 8421-8426, 2008.

[57] A. Göpferich, "Mechanisms of polymer degradation and erosion," *Biomaterials,* vol. 17, no. 2, pp. 103-114, 1996.

[58] C. R. Gajjar and M. W. King, "Degradation process," in *Resorbable Fiber-Forming Polymers for Biotextile Applications*, Springer International Publishing, 2017, pp. 7-10.

[59] K. S. Katti, "Biomaterials in total joint replacement," *Colloids and Surfaces B: Biointerfaces,* vol. 39, no. 13, pp. 133-142, 2004.

[60] S. Lyu and D. Untereker, "Degradability of Polymers for Implantable Biomedical Devices," *International Journal of Molecular Sciences,* vol. 10, no. 9, pp. 4033-4065, 2009.

[61] F.-D. Kopinke, M. Remmler, K. Mackenzie, M. Möder and O. Wachsen, "Thermal decomposition of biodegradable polyesters-II. Poly(lactic acid)," *Polymer Degradation and Stability,* vol. 53, no. 3, pp. 329-342, 1996.

[62] J. Thomas, "Fundamental aspects of the radiolysis of solid polymers, crosslinking and degradation," *Nuclear Instruments and Methods in Physics Research Section B: Beam Interactions with Materials and Atoms,* vol. 265, no. 1, pp. 1-7, 2007.

[63] H. S. Azevedo and R. L. Reis, "Understanding the enzymatic degradation of biodegradable polymers and strategies to control their degradation rate," in *Biodegradable systems in tissue engineering and regenerative medicine*, CRC Press, 2005, p. 180.

[64] R. Langer and N. Peppas, "Chemical and Physical Structure of Polymers as Carriers for Controlled Release of Bioactive Agents: A Review," *Journal of Macromolecular Science, Part C,* vol. 23, no. 1, pp. 61-126, 1983.

[65] O. S. Kluin, "Antibiotic-loaded poly(trimethylene carbonate) degradation, release and staphylococcal biofilm inhibition," Groningen, 2016.

[66] B. Baroli, "Photopolymerization of biomaterials: issues and potentialities in drug delivery, tissue engineering, and cell encapsulation applications," *Journal of Chemical Technology and Biotechnology,* vol. 81, no. 4, p. 491–499, 2006.

[67] E. Blasco, M. Wegener and C. Barner-Kowollik, "Photochemically Driven Polymeric Network Formation: Synthesis and Applications," *Advanced Materials,* vol. 29, no. 15, p. 1604005, 2017.

[68] V. Kumbaraci, N. Talinli and Y. Yagci, "Photoinduced Crosslinking of Polymers Containing Pendant Hydroxyl Groups by Using Bisbenzodioxinones," *Macromolecular Rapid Communication,* vol. 28, no. 1, p. 72–77, 2007.

[69] Y. Yagci, S. Jockusch and N. J. Turro, "Photoinitiated Polymerization: Advances, Challenges, and Opportunities," *Macromolecules,* vol. 43, no. 15, p. 6245–6260, 2010.

[70] H. Shin, J. S. Temenoff and A. G. Mikos, "In Vitro Cytotoxicity of Unsaturated Oligo[poly(ethylene glycol) fumarate] Macromers and Their Cross-Linked Hydrogels," *Biomacromolecules,* vol. 4, no. 4, p. 552–560, 2003.

[71] A. S. Sarvestani, W. Xu, . X. He and E. Jabbari, "Gelation and degradation characteristics of in situ photo-crosslinked poly(l-lactide-co-ethylene oxide-co-fumarate) hydrogels," *Polymer,* vol. 48, no. 24, pp. 7113-7120, 2007.

[72] W. Bai, Z.-p. Zhang, Q. Li, D.-L. Chen, H.-C. Chen, N. Zhao and C.-D. Xiong, "Miscibility, morphology and thermal properties of poly(para-dioxanone)/poly(D,L-lactide) blends," *Polymer International,* vol. 58, no. 2, pp. 183-189, 2009.

[73] K. L. Garvin, J. A. Miyano, D. Robinson, D. Giger, J. Novak and S. Radio, "Polylactide/polyglycolide antibiotic implants in the treatment of osteomyelitis. A canine model.," *The Journal of Bone and Joint Surgery,* vol. 76, no. 10, pp. 1500-1506, 1994.

[74] A. G. Ding and S. P. Schwendeman, "Acidic microclimate pH distribution in PLGA microspheres monitored by confocal laser scanning microscopy," *Pharmaceutical Research,* vol. 25, no. 9, pp. 2041-2052, 2008.

[75] M. Taylor, A. U. Daniels , K. P. Andriano and J. Heller, "Six bioabsorbable polymers: in vitro acute toxicity of accumulated degradation products," *Journal of Applied Biomaterials,* vol. 5, no. 2, pp. 151-157, 1994.

[76] O. Bostman, E. Hirvensalo, J. Makinen and P. Rokkanen, "Foreign-body reactions to fracture fixation implants of biodegradable synthetic polymers," vol. 72, no. 4, pp. 592-596, 1990.

[77] Z. Zhang, R. Kuijer, S. K. Bulstra, D. W. Grijpma and J. Feijen, "The in vivo and in vitro degradation behavior of poly(trimethylene carbonate)," *Biomaterials,* vol. 27, no. 9, pp. 1741-1748, 2006.

[78] A. Pego, M. J. A. Van Luyn, L. A. Brouwer, P. B. v. Wachem, A. A. Poot, D. W. Grijpma and J. Feijen, "In vivo behavior of poly(1,3-trimethylene carbonate) and copolymers of 1,3-trimethylene carbonate with D,L-lactide or epsilon-caprolactone: Degradation and tissue response," *Journal of Biomedical Materials Research Part A,* vol. 67, no. 3, pp. 1044-1054, 2003.

[79] R. P. Brannigan and A. P. Dove, "Synthesis, properties and biomedical applications of hydrolytically degradable materials based on aliphatic polyesters and polycarbonates," *Biomaterials Science,* vol. 5, no. 1, pp. 9-21, 2017.

[80] D. J. Darensbourg, A. Horn Jr and A. I. Moncada, "A facile catalytic synthesis of trimethylene carbonate from trimethylene oxide and carbon dioxide," *Green Chemistry,* vol. 12, no. 8, p. 1376–1379, 2010.

[81] C. J. Whiteoak, N. Kielland, V. Laserna, E. C. Escudero-Adan, E. Martin and A. W. Kleij, "A Powerful Aluminum Catalyst for the Synthesis of Highly Functional Organic Carbonates," *Journal of the American Chemical Society,* vol. 135, no. 4, pp. 1228-1231, 2013.

[82] I. Engelberg and J. Kohn, "Physico-mechanical properties of degradable polymers used in medical applications: A comparative study," *Biomaterials,* vol. 12, no. 3, pp. 292-304, 1991.

[83] K. J. Zhu, R. W. Hendren, K. Jensen and C. G. Pitt, "Synthesis, properties, and biodegradation of poly(1,3-trimethylene carbonate)," *Macromolecules,* vol. 24, no. 8, pp. 1736-1740, 1991.

[84] A. P. Pego, D. W. Grijpma and J. Feijen, "Enhanced mechanical properties of 1,3-trimethylene carbonate polymers and networks," *Polymer,* vol. 44, no. 21, pp. 6495-6504, 2003.

[85] A. Pego, B. Siebum, M. Van Luyn, X. Gallego y Van Seijen, A. Poot AA, D. Grijpma and J. Feijen, "Preparation of degradable porous structures based on 1,3-trimethylene carbonate and D,L-lactide (co)polymers for heart tissue engineering," *Tissue Engineering,* vol. 9, no. 5, pp. 981-994, 2003.

[86] R. Chapanian, M. Y. Tse, S. C. Pang and B. G. Amsden, "The role of oxidation and enzymatic hydrolysis on the in vivo degradation of trimethylene carbonate based photocrosslinkable elastomers," *Biomaterials,* vol. 30, no. 3, p. 295–306, 2009.

[87] A. P. Pego, A. A. Poot and D. W. Grijpma, "In Vitro Degradation of Trimethylene Carbonate Based (Co)polymers," *Macromolecular Bioscience,* vol. 2, no. 9, pp. 411-419, 2001.

[88] Q. Liu, L. Jiang, R. Shi and L. Zhang, "Synthesis, preparation, in vitro degradation, and application of novel degradable bioelastomers—A review," *Progress in Polymer Science,* vol. 37, no. 5, pp. 715-765, 2010.

[89] C. Sanson, C. Schatz, J.-F. Le Meins, A. Brulet, A. Soum and S. Lecommandoux, "Biocompatible and Biodegradable Poly(trimethylene carbonate)-b-Poly (L-glutamic acid) Polymersomes: Size Control and Stability," *Langmuir Article,* vol. 26, no. 4, p. 2751–2760, 2010.

[90] H. Oliveira, J. Theveno, E. Garanger, E. Ibarboure, P. Calvo, P. Aviles, M. J. Guillen and S. Lecommandoux, "Nano-Encapsulation of Plitidepsin: In Vivo Pharmacokinetics, Biodistribution, and Efficacy in a Renal Xenograft Tumor Model," *Pharmaceutical Research,* vol. 31, p. 983–991, 2014.

[91] D. Bacinello, E. Garanger, D. Taton, K. C. Tam and S. Lecommandoux, "Tailored drug-release from multi-functional polymer-peptide hybrid vesicles," *European Polymer Journal,* vol. 62, pp. 363-373, 2015.

[92] X. Jiang, X. Sha, H. Xin, X. Xu, J. Gu, W. Xia, C. Shuo, X. Yike, L. Chen, Y. Chen and X. Fang, "Integrin-facilitated transcytosis for enhanced penetration of advanced gliomas by poly(trimethylene carbonate)-based nanoparticles encapsulating paclitaxel," *Biomaterials,* vol. 34, no. 12, pp. 2969-2979, 2013.

[93] X. Jiang, X. Sha, . H. Xin, L. Chen, X. Gao, X. Wang, K. Law, J. Gu, Y. Chen, Y. Jiang, X. Ren, Q. Ren and X. Fang, "Self-aggregated pegylated poly (trimethylene carbonate) nanoparticles decorated with c(RGDyK) peptide for targeted paclitaxel delivery to integrin-rich tumors," *Biomaterials,* vol. 32, pp. 9457-9469, 2011.

[94] X. Jiang, H. Xin, J. Gu, F. Du, C. Feng, Y. Xie and X. Fang, "Enhanced Antitumor Efficacy by D-Glucosamine-Functionalized and Paclitaxel-Loaded Poly(Ethylene Glycol)-Co-Poly(Trimethylene Carbonate) Polymer Nanoparticles," *Journal of Pharmaceutical Sciences,* vol. 103, no. 5, pp. 1487-1496, 2014.

[95] X. Jiang, H. Xin, Q. Ren, J. Gu, L. Zhu, F. Du, C. Feng, Y. Xie, X. Sha and X. Fang, "Nanoparticles of 2-deoxy-d-glucose functionalized poly(ethylene glycol)-co-poly(trimethylene carbonate) for dual-targeted drug delivery in glioma treatment," *Biomaterials,* vol. 35, no. 1, pp. 518-529, 2014.

[96] S. H. Kim, J. P. Tan, F. Nederberg, K. Fukushima, J. Colson, C. Yang, A. Nelson, Y.-Y. Yang and J. L. Hedrick, "Hydrogen bonding-enhanced micelle assemblies for drug delivery," *Biomaterials,* vol. 31, no. 31, pp. 8063-8071, 2010.

[97] S. J. Buwalda, L. B. Perez, S. Teixeira, L. Calucci, C. Forte, J. Feijen and P. J. Dijkstra, "Self-Assembly and Photo-Cross-Linking of Eight-Armed PEG-PTMC Star Block Copolymers," *Biomacromolecules,* vol. 12, p. 2746–2754, 2011.

[98] X. Wang, Y. Yang, H. Jia, W. Jia, S. Miller, B. Bowman, J. Feng and F. Zhan, "Peptide decoration of nanovehicles to achieve active targeting and pathology-responsive cellular uptake for bone metastasis chemotherapy," *Biomaterial Science,* vol. 2, no. 7, pp. 961-972, 2014.

[99] J. Jansen, G. Mihov, J. Feijen and D. W. Grijpma, "Photo-Crosslinked Biodegradable HydrogelsPrepared From Fumaric Acid Monoethyl Ester-Functionalized Oligomers for Protein Delivery," *Macromolecular Bioscience,* vol. 12, no. 5, p. 692–702, 2012.

[100] A. K. Sen, "Roll Coating," in *Coated Textiles: Principles and Applications*, CRC Press, 2008, pp. 77-78.

[101] J. R. Wagner, "Coating Applications," in *Multilayer Flexible Packaging*, Elsevier, 2016, p. 215.

[102] Y. Tian, X. Zhang, H.-Z. Geng, H.-J. Yang, C. Li, S.-X. Da, X. Lu, J. Wang and S.-L. Jia, "Carbon nanotube/polyurethane films with high transparency, low sheet resistance and strong adhesion for antistatic application," *RCS Advances,* vol. 7, p. 53018–53024, 2017.

[103] S. Azoz, A. L. Exarhos, A. Marquez, L. M. Gilbertson, S. Nejati, J. J. Cha, J. B. Zimmerman, J. M. Kikkawa and L. D. Pfefferle, "Highly Conductive Single-Walled Carbon Nanotube Thin Film Preparation by Direct Alignment on Substrates from Water Dispersions," *Langmuir,* vol. 31, p. 1155−1163, 2015.

[104] J. Scheirs, Ed., Modern fluoropolymers: High performance polymers for diverse applications, New York: John Wiley & Sons, Inc., 1997.

[105] S. S. Williams, S. Retterer, R. Lopez, R. Ruiz, E. T. Samulski and J. M. DeSimone, "High-Resolution PFPE-based Molding Techniques for Nanofabrication of High-Pattern Density, Sub-20 nm Features: A Fundamental Materials Approach," *Nano Letters,* vol. 10, no. 4, pp. 1421-28, 2010.

[106] D. A. Canelas, . K. P. Herlihy and J. M. DeSimone, "Top-Down Particle Fabrication: Control of Size and Shape for Diagnostic Imaging and Drug Delivery," *Wiley Interdisciplinary Reviews: Nanomedicine and Nanobiotechnology,* vol. 1, no. 4, p. 391–404, 2009.

[107] D. M. Toriumi, W. F. Raslan, M. Friedman and E. Tardy, "Histotoxicity of Cyanoacrylate Tissue Adhesives: A Comparative Study," *Archives of Otolaryngology Head and Neck Surgery,* vol. 116, no. 5, pp. 546-550, 1990.

[108] Y. Geng, P. Dalhaimer, S. Cai, R. Tsai, M. Tewari, T. Minko and D. E. Discher, "Shape effects of filaments versus spherical particles in flow and drug delivery," *Nature Nanotechnology,* vol. 2, no. 4, pp. 249-255, 2007.

[109] Q. Hou, D. W. Grijpma and J. Feijen, "Creep-resistant elastomeric networks prepared by photocrosslinking fumaric acid monoethyl ester-functionalized poly(trimethylene carbonate) oligomers," *Acta Biomaterialia,* vol. 5, no. 5, p. 1543–1551, 2009.

[110] T. Matsuda, I. K. Kwon and S. Kidoak, "Photocurable biodegradable liquid copolymers: synthesis of acrylate-end-capped trimethylene carbonate-based prepolymers, photocuring, and hydrolysis.," *Biomacromolecules,* vol. 5, no. 2, p. 295–305, 2004.

[111] F. P. Melchels, J. Feijen and D. W. Grijpma, "A poly(D,L-lactide) resin for the preparation of tissue engineering scaffolds by stereolithography," *Biomaterials,* vol. 30, no. 23-24, pp. 3801-3809, 2009.

[112] A. O. Helminen, H. Korhonen and J. V. Seppala, "Crosslinked poly(ester anhydride)s based on poly(ε-caprolactone) and polylactide oligomers," *Journal of Polymer Science: Part A: Polymer Chemistry,* vol. 41, no. 23, p. 3788–3797, 2003.

[113] J. P. Fisher, M. D. Timmer, T. A. Holland, D. Dean, P. S. Engel and A. G. Mikos, "Photoinitiated Cross-Linking of the Biodegradable Polyester Poly(propylene fumarate). Part I. Determination of Network Structure," *Biomacromolecules,* vol. 4, no. 5, p. 1327–1334, 2003.

[114] A. S. Sawhney, C. P. Pathak and J. A. Hubbell, "Bioerodible Hydrogels Based on Photopolymerized Poly(ethylene glycol)-co-poly(a-hydroxyacid) Diacrylate Macromers," *Macromolecules,* vol. 26, no. 4, pp. 581-587, 1993.

[115] K. Garvin and C. Feschuk, "Polylactide-polyglycolide antibiotic implants," *Clinical Orthopaedics and Related Research,* vol. 437, pp. 105-110, 2005.

[116] Z. Zhang, D. Grijpma and J. Feijen, "Trimethylene carbonate-based polymers for controlled drug delivery applications," *Journal of Controlled Release,* vol. 116, no. 2, pp. e28-e29, 2006.

[117] K. Koga, A. Sudo and T. Endo, "Revolutionary phosgene-free synthesis of α-amino acid N-carboxyanhydrides using diphenyl carbonate based on activation of α-amino acids by converting into imidazolium salts," *Journal of Polymer Science, Part A: Polymer Chemistry,* vol. 48, no. 19, pp. 4351-4355, 2010.

[118] A. P. Pego,, C. L. A. M. Vleggeert-Lankam, M. Deenen,, E. A. J. F. Lakke, D. W. Grijpma, and A. A. Poot, "Adhesion and growth of human Schwann cells on trimethylene carbonate (co)polymers," *Journal of Biomedical Materials Research Part A*, vol. 67A, no. 3, pp. 876-885, 2003.

[119] D. W. Grijpma, Q. Hou and J. Feijen, "Preparation of biodegradable networks by photo-crosslinking lactide, epsilon-caprolactone and trimethylene carbonate-based oligomers functionalized with fumaric acid monoethyl ester," *Biomaterials*, vol. 26, no. 16, pp. 2795-2802, 2005.

[120] R. Alagirusamy and A. Das, "Methods and Machinery for Yarn Coating," in *Technical Textile Yarns: Industrial and Medical Applications*, Cambridge, CRC Press, 2010, pp. 170-173.

[121] A. S. Diamond and D. S. Weiss, "Solvent Coating Machine," in *Handbook of Imaging Materials*, Marcel Dekker Inc., 2002, pp. 132-134.

[122] L. G. Albano, M. H. Boratto, O. Nunes-Neto and C. F. Graeff, "Low voltage and high frequency vertical organic field effect transistor based on rod-coating silver nanowires grid electrode," *Organic Electronics*, vol. 50, pp. 311-316, 2017.

[123] H.-G. Cheong, J.-H. Kim, J.-H. Song, U. Jeong and J.-W. Park, "Highly flexible transparent thin film heaters based on silver nanowires and aluminum zinc oxides," *Thin Solid Films*, vol. 589 , p. 633–641, 2015.